

Chapter 1

Introduction to Transmission Lines and Their Application to Electromagnetic Phenomena

In recent years, an exciting new branch of research activity has emerged, dealing with extremely fast phenomena in semiconductors and gases. The introduction of high speed instrumentation and devices, with time scales often in the 1 to 1000 picosecond range, has prompted the investigation of a variety of fast phenomena, including the generation of electromagnetic pulses and light, photoconductivity, avalanching, scattering, fast recombination, and many other physical processes. The research has been driven by several applications [1], [2]. These include ultra-wideband imaging and radar, as well as ultra-wideband communications (thus avoiding the use of wires or optical fibers). In addition, the availability of new, high speed instrumentation has provided researchers with a valuable tool for learning the fundamental properties of materials. In all the aforementioned applications, a central feature is the generation of electromagnetic pulses with either a narrow pulse duration or a fast risetime (or both). The short time interval involved (in either the risetime or the pulse duration), insures that a wide frequency spectrum is produced, a property which is essential for the cited applications.

The understanding of fast phenomena and ultra-wideband electromagnetic sources is made more complicated by the very fast risetimes and by the fact that the wavelength of the signals being produced are often smaller or comparable to the characteristic length of the device or experimental configuration under study. As a result the use of lumped circuit variables is inappropriate and we must use either transmission line variables or Maxwell's equations directly.

Electromagnetic signals with very short wavelength may be generated by a sudden transition in the conductivity of the medium. Suppose, for example, an electric field bias first is applied to the medium and that subsequently the conductivity of a portion of the medium is

suddenly increased (for example, by photoconductivity or avalanching). The sudden change in conductivity will generate electromagnetic pulses with very steep risetimes, thus producing short wavelength signals. In cases where light is produced (for example, when carriers recombine), the wavelength naturally will be smaller or at least comparable to the device size. In any event, the analyses often used to describe devices and experimental configurations do not adequately address the short wavelength signals which are generated, and subsequently dispersed throughout the device and the surrounding space. One should not underestimate the importance of the electromagnetic energy dispersal (which includes light signals). Often the physics of underlying processes are misunderstood because the electromagnetic energy dispersal, which delivers the physics to the detector, is not taken into account properly, particularly for fast phenomena. It is hoped the ensuing discussion will help to correct this deficiency and lead to a better understanding of the dispersal of ultra-wideband electromagnetic signals and associated phenomena.

In this volume we endeavor to describe fast electromagnetic phenomena, relying on iterative rate equations which use transmission line matrix (TLM) variables. As with comparable numerical techniques, such as the finite difference method, the transmission line element must be made very small in order to attain accuracy, and solutions at a given time step depend on a knowledge of solutions at a previous time step. In terms of physical interpretation and intuition, however, the TLM method is far superior to that of finite differences or other similar numerical techniques. The physical appeal of the TLM method may be viewed, in a conceptual way, from the two basic components which comprise the TLM matrix: the transmission lines and the nodes which form the intersection of the lines, as noted in Fig.1.1. TLM lines may be regarded as having spatial extent, whereas the nodes are regarded as infinitely small. With this model, we can conceptually separate the physics and energy dispersal of a given problem in electromagnetics. Using a simple picture, the nodes represent the physics, and the physical processes (such as conductivity changes) are mapped onto the nodes, which then control the flow of energy in the TLM lines. The TLM lines then are responsible for the energy distribution and storage. (However, as we shall see in later Chapters, the TLM lines are not entirely devoid of physics since the fields in these lines “interact” with one another, using quantum mechanical ideas, which affect propagation behavior).

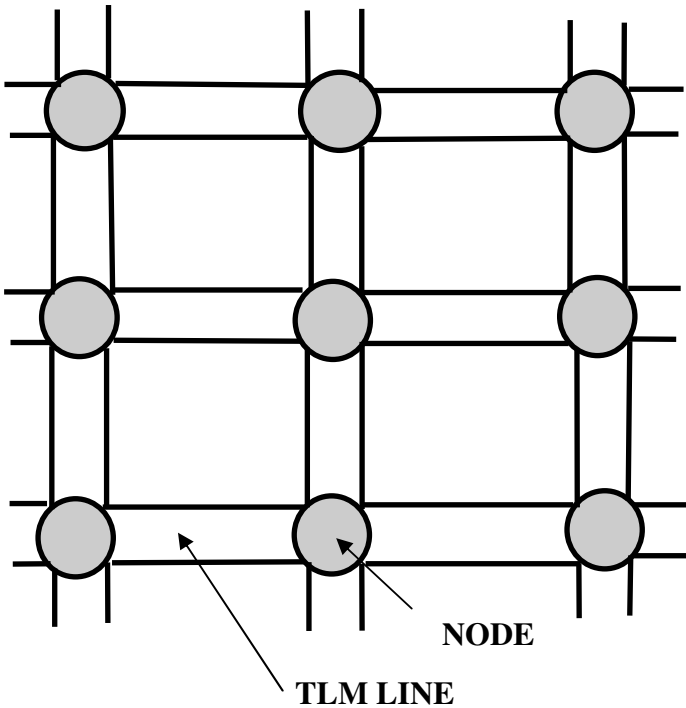


FIG. 1.1 CONCEPTUAL VIEW OF TRANSMISSION LINE (TLM) MATRIX CONSISTING OF NODES AND TLM LINES. IN MOST CASES, THESE TWO COMPONENTS HAVE SEPARATE FUNCTIONS: THE TLM LINES DISTRIBUTE THE EM ENERGY AND THE NODES CONTROL THE PHYSICS.

Within the electrical engineering community the use of transmission line variables to treat one dimensional electromagnetic problems has gained in popularity over the years. As a result, a certain comfort level has been attained by engineers in the use of transmission line terminology. The carryover of the TLM description to two and three dimensional electromagnetic problems, however, has not received the same attention. This may not be surprising, since the 2D and 3D treatments are more complicated and the 1D must be augmented and revised to a considerable degree. For example, the boundary conditions

at the nodes, for the 2D and 3D problems, result in more complicated scattering behavior. In addition the incorporation of concepts such as plane wave correlation and corrections for grid anisotropy, have not been applied to standard TLM theory, thus making the TLM approach, for 2D and 3D problems, less valuable. The necessary revisions for removing these defects, for 2D and 3D models, are described in detail in the ensuing Chapters. The revised theory retains the benefits of ease of interpretation in solving electromagnetic problems.

If the required transmission line elements (and the associated nodes) are not too large in number, then certain classes of problems, such as one dimensional microwave transformers and non-uniform TLM lines, as well as simple 2D problems, may be treated using commercially available software (without the aforementioned corrections). For this reason, SPICE, a well known example of such software, is discussed in Chapter 8 where we solve several types of TLM problems using this method.

1.1 Simple Experimental Example

The simple arrangement shown in Fig.1.2 will help to illustrate the concepts more easily. The Figure shows a side view of two electrodes separated by semiconductor material, with an electric field bias between the two electrodes. Suppose a limited region of the semiconductor, shown by the darkened region, is suddenly created (either with a light pulse or by a localized, fast avalanche breakdown). This will give rise to an electromagnetic disturbance and possibly a light pulse (depending on the medium), emanating from the conduction region. The dashed curve may be conceptually regarded as an equal amplitude contour of the electromagnetic disturbance at a given instant in time. As noted the disturbance is assumed to be asymmetric, since the amplitude will be more pronounced in the direction perpendicular to the bias field. One may regard the electromagnetic disturbance as a traveling wave created by that part of the initial field which is parallel to the surface of the activated conduction region. The wave, i.e., the disturbance, is reflected normally from the surface of the activation region while undergoing an electric field inversion, so that the total field, in the immediate vicinity of the initial conduction region, is partially or completely canceled (depending on the degree of conductivity). The situation changes, of course, if the initial wave disturbance undergoes an additional field reversal at the boundary

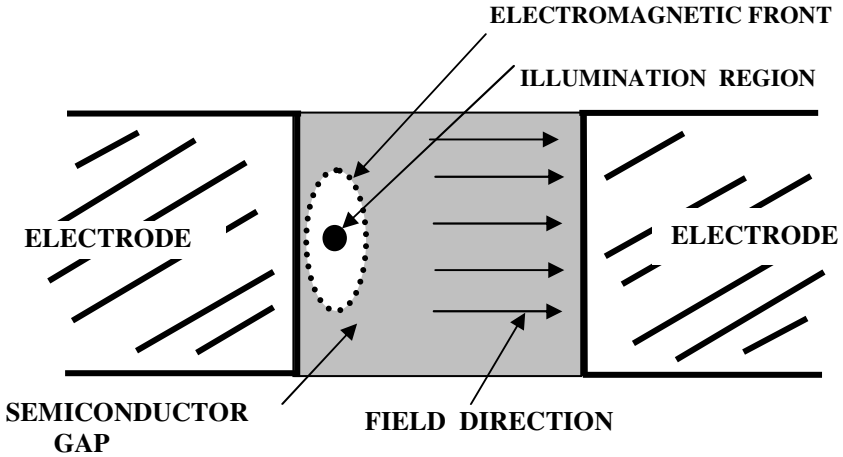


FIG. 1.2 CONCEPTUAL VIEW OF DISPLACEMENT CURRENT ARISING FROM ILLUMINATION OF A LIMITED PORTION OF A SEMICONDUCTOR GAP.

of a nearby conductor, which can be one of the two electrodes or some auxiliary conductor (such as the grounded member of a transmission line). Changes in the wave disturbance can also take place, of course, due to the existence of a dielectric interface.

The final result is a complex array of waves throughout the region, in which the field configuration depends on the temporal and spatial properties of the conduction region, as well as the device geometry. Given such conditions, the field will change dramatically (compared to the initial uniform, static field) and regions of field diminution or field enhancement are likely to occur.

In case light is produced in the semiconductor, the situation is in some ways easier to describe, and in other ways it is more complicated. The light disturbance profile will be more symmetric, compared to that of the electromagnetic front, because of the shorter wavelength and random nature of the recombination process. However, the front of the light signal will lag the electromagnetic front, with the delay depending on the recombination time. The main complication in handling light waves is the requirement of a higher resolution TLM matrix, as will be discussed in later Chapters.

As we shall see in subsequent discussions, the TLM method is extremely well suited to the description of conductivity generation in both solid-state and gaseous media. In semiconductors, for example, both the light and the electromagnetic fields will contribute to the possible extension of the original conductivity region. Suppose the semiconductor is illuminated with a light signal. The light signal can extend the conductivity by means of several processes, all of which are linked together. First, the light signal will create carriers via the direct photo-ionization. Second, the light may create sufficient seed carriers such that an avalanche is more easily triggered. Third, a spreading light signal, resulting from direct recombination in the original photo-ionized region, may also contribute to the extension of the conductivity region. Finally, even without direct carrier seeding, an avalanche may be produced in a region which is remote from the original site of the light impingement, caused by augmentation of the electromagnetic field (following the upset of the initial static field) in various regions. The TLM method is well suited for describing such a conductivity extension.

1.2 Examples of Impulse Sources

The types of electromagnetic problems which the TLM method can address have virtually no restrictions. We will discuss several generic impulse sources which have stimulated the development of the TLM method. It should be mentioned, however, that in mostly all the examples using the TLM method, cited here and throughout the book, the conductivity generation occurs by means of a light pulse impinging on a semiconductor, with the carriers produced by direct photo-ionization. This is merely a convenience, and it should be borne in mind that any other source of conductivity (such as avalanching or carrier injection) may be incorporated into the TLM formulation.

As a first example, Fig.1.3, consider a parallel plate transmission line in which a portion of the upper conductor has been removed and substituted with a semiconductor, capable of holding off voltage. The line is then charged up to voltage, producing a field, as indicated in the semiconductor, as well as a fringing field between the two conductors. The sudden creation of carriers with a light pulse, throughout the entire semiconductor, or even in a limited portion of the semiconductor, then produces a fast risetime pulse which travels down the line toward the

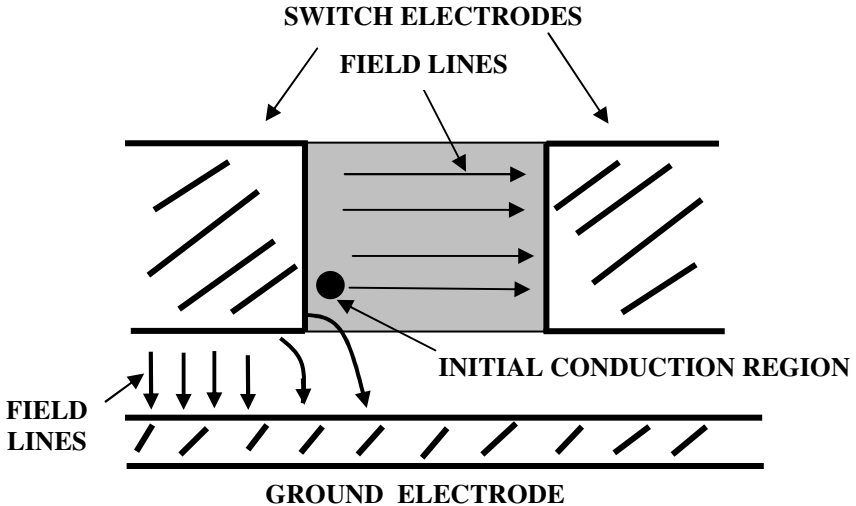


FIG. 1.3 EXTENSION OF CONDUCTIVITY REGION FOLLOWING ILLUMINATION NEAR ELECTRODE. SEMICONDUCTOR GAP INTERRUPTS UPPER CONDUCTOR OF TRANSMISSION LINE.

output, typically an antenna. The TLM method may then be used to determine the instantaneous field profiles throughout the entire device region, which includes the dielectric as well as the semiconductor regions. If so desired we also may apply the TLM analysis to the dielectric region above the semiconductor as well. Indeed, during the “commutation” time, some electromagnetic energy will radiate out from the semiconductor. The TLM analysis and computation may be extended in straightforward fashion to determine the radiated signal during commutation. Another impulse source, which combines the functions of the energy storage, antenna, and the switch is shown in Fig.1.4. The initial electrostatic energy is stored with a bias voltage between the conductors of a strip transmission line. The conductors diverge as shown to form a composite transformer/antenna. The switch, in the form of an optically activated semiconductor, is situated at the low impedance end of the transformer. When the semiconductor is suddenly activated by a narrow pulse laser, an inverted pulse is launched toward the output of the

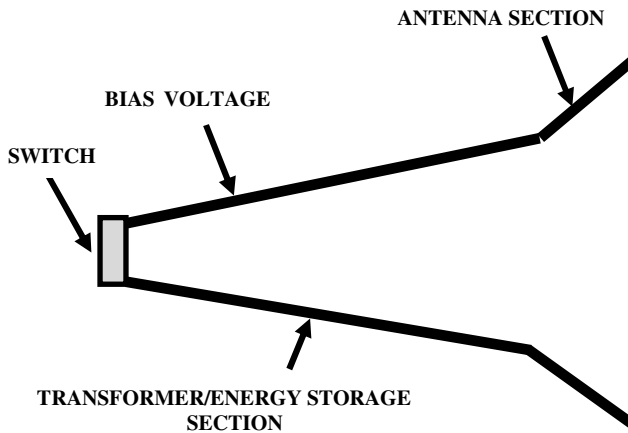


FIG. 1.4 PULSE SOURCE CONSISTING OF A SWITCH AT THE LOW IMPEDANCE SIDE OF A TRANSFORMER, WHICH ALSO STORES THE ELECTROSTATIC ENERGY AND COUPLES TO AN ANTENNA.

antenna. The TLM method then may be used to determine the fields throughout the entire space, i.e., the semiconductor, transformer and radiation regions. Of course there are many other versions of impulse sources. Another version consists of tapered electrodes deposited on a semiconductor substrate. If a voltage is placed between the electrodes and the gap region optically activated by a narrow pulse laser, a transient oscillation is set up, much like a Hertzian dipole, causing a short electromagnetic burst of energy to be radiated. Once again TLM methods may be employed for the various regions of interest.

One can surmise that obtaining practical, quantitative, and accurate electromagnetic solutions for the above configurations would appear to be a formidable task, especially if one must rely solely on numerical analysis, based on Maxwell's equations, the boundary conditions, as well as the physics underlying various phenomena such as photoconductivity, avalanching, recombination, etc... The purpose of this book is to invoke an alternative method, the TLM approach, which from a mathematical point of view has close links to standard numerical techniques but which is far superior in terms of its ease of physical interpretation and flexibility. The new method relies on transmission

line variables, concepts which are readily familiar among many research workers, to describe the behavior of the medium. As mentioned previously, the medium is represented by an imaginary matrix of transmission lines, wherein the energy storage and dispersal is taken into account by the transmission lines and the all physical processes (except for the energy dispersal, which also includes wave correlations discussed later) are mapped onto the nodes, i.e., the intersection of the transmission lines. An outline of the transmission line model, and its relationship to standard numerical techniques, using finite differences, is described in the following Sections.

1.3 Model Outline

The development of the transmission line model starts with Maxwell's wave equation [3], including the conductivity term (MKS units are employed). Thus,

$$\nabla^2 \mathbf{E} - (1/v^2)(\partial^2 \mathbf{E}/\partial t^2) - \mu\sigma(\partial \mathbf{E}/\partial t) = 0 \quad (1.1)$$

where: \mathbf{E} = Electric Field
 t = time
 μ = permeability
 v = propagation velocity
 σ = conductivity

Eq.(1.1) assumes there is no true charge in the medium. A similar equation also holds for the magnetic field. As mentioned previously, numerical methods may be used to obtain solutions to Eq.(1.1). Instead of following this path, however, a transmission line approach is investigated. Toward this goal, it is convenient to first consider the one dimensional case. Accordingly, the wave equation then becomes

$$\partial^2 \mathbf{E}/\partial x^2 - (1/v^2)(\partial^2 \mathbf{E}/\partial t^2) - \mu\sigma(\partial \mathbf{E}/\partial t) = 0 \quad (1.2)$$

where x is the distance along the propagation direction and \mathbf{E} is transverse to the propagation. An important time constant associated with the wave equation is the relaxation time, ϵ/σ , where ϵ is the permittivity. The relaxation time will determine the choice of our cell size, denoted by

length Δl . In order to minimize losses over the cell length, and thus provide the necessary resolution and numerical convergence, the cell propagation time, $\Delta l/v$, should be much smaller than the relaxation time, ϵ/σ . Δl therefore should satisfy $\Delta l \ll \epsilon v/\sigma$. In addition, Δl should be much smaller than any characteristic length associated with, for example, the geometry or other experimental condition. Obviously, the smaller the size of the cell size, the greater the resolution, although this places a greater burden on computer speed and memory.

Equation (1.2) is identical to the well known transmission line equation, which governs the voltage V for a one dimensional transmission line using circuit variables, as shown Fig.1.5,

$$\partial^2 V^2 / \partial x^2 - (L' C') (\partial^2 V / \partial t^2) - L' G' (\partial V / \partial t) = 0 \quad (1.3)$$

Eq.(1.3) is derived from the usual relationships between voltage and current, taking into account the circuit parameters of capacitance, inductance, and conductance (see for example reference [4]). Besides the inductance per unit length, L' , and capacitance per unit length, C' , there is included a shunt conductance per unit length, G' . G' accounts for losses between conductors, e.g., the presence of carriers in a semiconductor medium. Equation (1.3) is important because of the familiarity of the circuit variables, several of which we will use during the subsequent discussion.

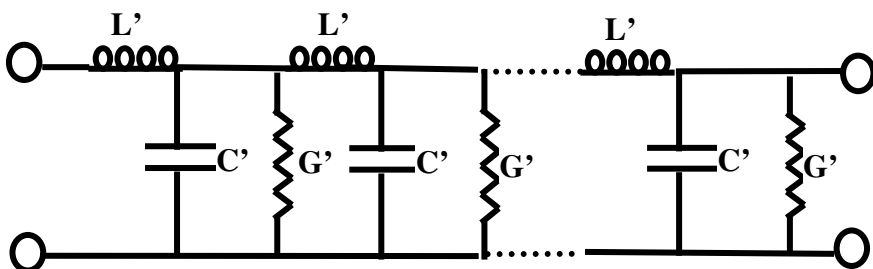


FIG. 1.5 ONE DIMENSIONAL CIRCUIT CELL CONSISTING OF LUMPED CIRCUIT PARAMETERS.

TABLE 1.1 CORRESPONDENCE BETWEEN WAVE AND CIRCUIT VARIABLES		
	ELECTROMAGNETIC VARIABLE	CIRCUIT VARIABLE
FIELD	E	V
PERMITTIVITY	ϵ	C'
PERMEABILITY	μ	L'
CHARACTERISTIC IMPEDANCE	$\{\mu/\epsilon\}^{1/2}$	$\{L'/C'\}^{1/2}$
PROPAGATION VELOCITY	$\{\mu \epsilon\}^{-1/2}$	$\{L'C'\}^{-1/2}$
LOSS	σ	G'
RELAXATION TIME	$\{\epsilon/\sigma\}$	C'/G'

Table 1.1 exhibits the relationship between the wave equation using field variables, Eq.(1.2), and that using circuit variables, Eq.(1.3). An important simplification occurs when we select a small transmission line element (or cell) of length Δl . It is useful to state the total capacitance, inductance, and conductance associated with the line element, which we identify as

$$C = C' \Delta l = \epsilon \Delta l \tag{1.4a}$$

$$L = L' \Delta l = \mu \Delta l \tag{1.4b}$$

$$G = G' \Delta l = \sigma \Delta l \tag{1.4c}$$

The total resistance R of the element is thus $R=1/G$. The relaxation time, ϵ/σ , is equal to the “RC” discharge time for the cell, as noted from Eq.(1.4). We also identify the impedance of the line as

$$Z_0 = (\mu/\epsilon)^{1/2} = (L'/C')^{1/2} \quad (1.5)$$

At this point we can quantify the selection of Δl . In the presence of conductivity, better accuracy is ensured when we select Δl such that

$$\Delta l \ll v(\epsilon/\sigma) = v(C'/G') = v(RC) \quad (1.6)$$

where

$$v = (\mu\epsilon)^{-1/2} = (L'C')^{-1/2} \quad (1.7)$$

Eqs.(1.6)-(1.7) state that the transit time delay in cell Δl , equal to $\Delta l/v$, is much smaller than the RC time of the cell. An equivalent statement is that the lumped resistance, R , of the element Δl is much larger than the characteristic impedance, Z_0 , or

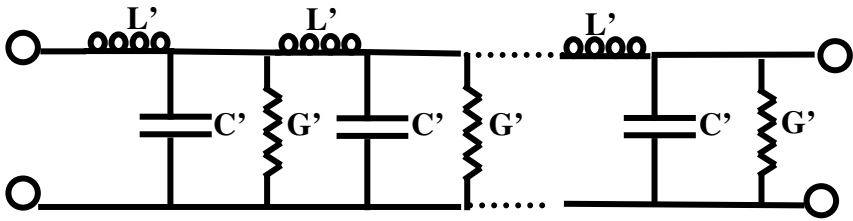
$$R \gg Z_0 \quad (1.8)$$

By virtue of previous equations, L' , C' may be combined into a lossless transmission element, Z_0 , and the conductance may be combined into *two* resistors, R , located at the ends of the transmission line, as shown in Fig.1.6, where R is given by

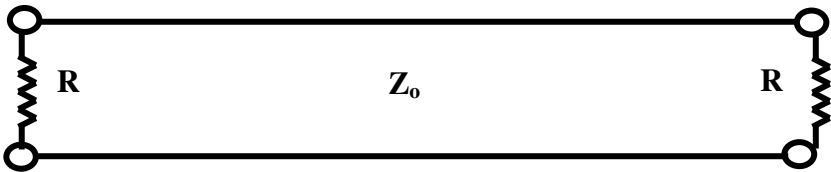
$$R = 2/\sigma\Delta l = 2/G'\Delta l \quad (1.9)$$

A two factor appears in Eq.(1.9) since each of the two resistors, R , may be considered in parallel. Another way to view the introduction of the two factor is the following. By focusing on a single TLM line element, we ignore the adjoining TLM elements, each with similar end resistors; since such adjoining resistors are in parallel, a two factor should be introduced when “extracting” a single element from the chain.

The previous discussion has focused on a single isolated cell. We must now consider a linear chain of such cells as in Fig.1.7, consisting of coupled transmission line elements with lumped end resistors, $R'=2/\sigma\Delta l$, where we append a prime in Fig. 1.7 to indicate R' belongs to that of



ONE DIMENSIONAL CELL CONSISTING OF LUMPED CIRCUIT PARAMETERS



ONE DIMENSIONAL CELL CONSISTING OF A TRANSMISSION ELEMENT Z_0 OF LENGTH Δl WITH SHUNT RESISTORS $R=2/\sigma\Delta l$.

FIG. 1.6 TRANSITION FROM LUMPED CIRCUIT CELL TO TRANSMISSION LINE CELL.

an isolated line element (prime not to be confused with per length). For uniform line segments, Fig.1.7(a), the coupled cells will have identical end resistors and at each junction, as alluded to previously, the parallel resistors are combined into $R = R'/2 = 1/\sigma\Delta l$ where R' is given by $2/\sigma\Delta l$. Now suppose the cell chain is non-uniform, noted in Fig.1.7(b), so that adjacent cells have unequal resistivities (but the same dielectric constant). For this line, the conductances at each node will add and thus the corresponding resistors will add in parallel fashion, so that the combined resistance, R_{12} , satisfies $R_{12} = R_1 R_2 / (R_1 + R_2)$. As with the uniform line, R_1 and R_2 satisfy the isolated cell expressions, $R_1 = 2/\sigma_1\Delta l$ and $R_2 = 2/\sigma_2\Delta l$. At this point the characterization of the chain is complete, and one may invoke the transient theory for transmission lines.

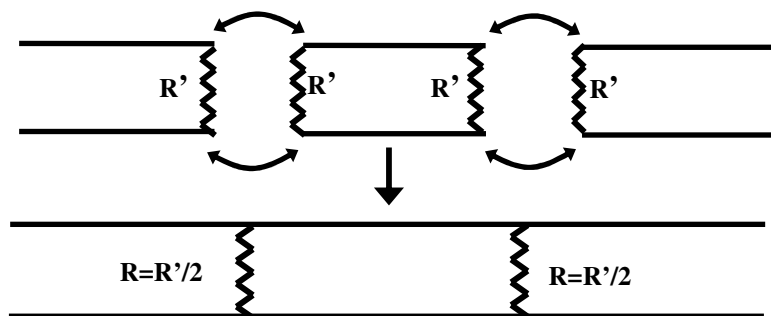


FIG. 1.7a COMBINING OF IDENTICAL 1D CELLS. $R = 1/\sigma\Delta l$.

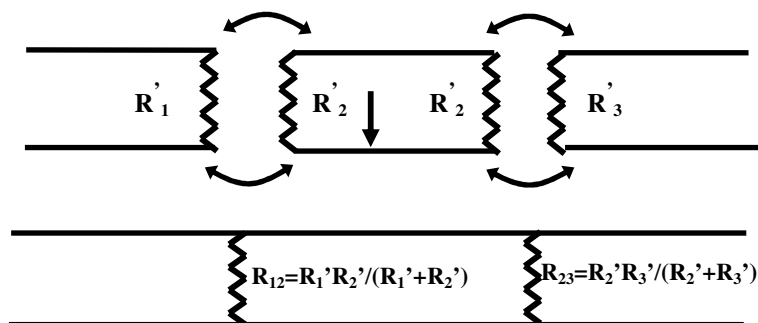


FIG. 1.7b COMBINING OF CELLS WITH UNEQUAL RESISTIVITY.

The resistance, R , initially very large, is activated when, for example, the effects of photoconductivity or avalanching occur. Once the cells are activated, propagation losses become important and we may then utilize transmission line theory to determine the response. These types of problems will be discussed quantitatively in the ensuing Chapters.

Although the circuits in Fig.1.7 are useful for understanding the basic concepts, two important flaws exist. For one thing the circuit is one dimensional and it does not take into account conductivity and electromagnetic spreading in the transverse directions. The second flaw, again

related to the one dimensional nature of the circuit, has to do with the lack of a stable solution during equilibrium, i.e., prior to the activation of the cells, when R or R_{12} , R_{23} , etc... are very large. Suppose each of the cells in Fig.1.7, which are connected in series, is initially charged to a different voltage. The cells will discharge into one another, unless artificial means are taken to prevent such a discharge, such as the artificial insertion of a series switch. A self consistent way to preserve equilibrium, prior to activation, is to insert an orthogonal transmission line in series; this then converts the one dimensional circuit into a 2D one. A similar extension to 3D also preserves the equilibrium. Before proving these assertions, we briefly describe the 2D and 3D arrays. This will be followed by background discussion in transmission line theory, which will allow us to place our previous claims on a firmer footing.

Figure 1.8 shows the circuit matrix used to describe electromagnetic and conductivity spreading in two dimensions. One way to view the circuit cell is to note that there are four square cells, with each region constant in voltage (V_1 , V_2 , V_3 , and V_4) but generally differing in value from the neighboring cell. The square regions, therefore, may be considered as conductors. Separating the constant voltage regions are the transmission lines, situated in the border region. The widths of the TLM lines are *exaggerated* for clarity. In this case the line impedances, Z_o , are the same. Initially the lines will be charged up to a voltage value equal to the voltage difference between adjacent cells. Note that the node resistance R is located at the hub of the matrix and actually consists of four identical resistors, R , each terminating one of the four TLM lines. It is worthwhile to realize that any signal arriving at the node will be equally scattered among the four transmission lines (in the absence of any significant conductivity). This property is similar to that in electromagnetics, in which each region of the wave front may be regarded as a point source. A similar extension of the circuit may be made to three dimensions. In 3D, however, the iso-potential regions are cubical, and there are eight cubes centered about each node point (Fig.1.9) and the TLM lines run along the edges. Also, for 3D, there are two independent, orthogonal fields and transmission lines associated with each cube edge.

Just as with the 1D case, the node and TLM line properties for 2D and 3D matrices are averaged over neighboring cells. Using cellular notation a detailed description of 1D, 2D, and 3D matrices is given in Chapters 2-3.

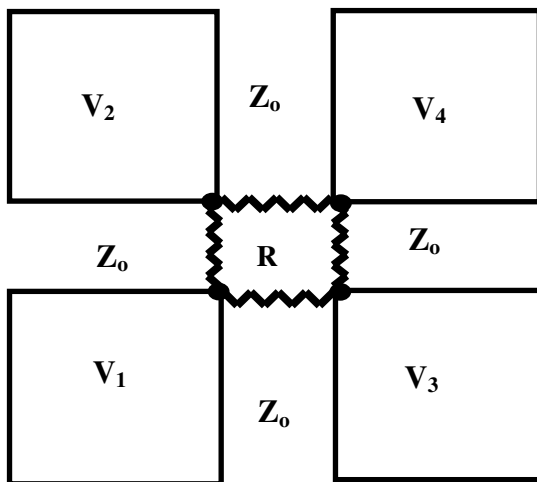


FIG. 1.8 TWO DIMENSIONAL MATRIX CONSISTING OF NODE AT CENTER OF FOUR ISO-POTENTIAL CELLS, SEPARATED BY TLM LINES Z_0 . WIDTH OF Z_0 IS EXAGGERATED.

NODE OF HIGHLIGHTED CELL

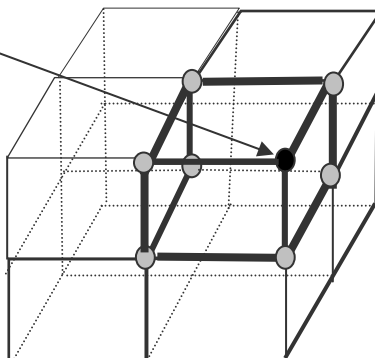
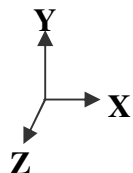


FIG. 1.9 THREE DIMENSIONAL MATRIX SHOWING EIGHT CELLS AND THEIR ASSOCIATED NODES. THE DARKENED NODE IS ASSOCIATED WITH THE HIGHLIGHTED CELL.

1.4 Application of Model to Small Node Resistance

We have adopted a model in which the cell node resistance is much larger than the cell line impedance. Stated another way, we impose the condition that the transit time of the cell Δt is much smaller than the RC time constant. Bear in mind that we can always satisfy this requirement by choosing a small enough cell size, Δl , for a given conductivity in the medium. Once conductivity is introduced among voltage biased cells, the cell voltages decay in a uniform fashion. In a simplified way, the situation may be depicted in terms of decaying waves (in both directions), which eventually vanish once a sufficient number of cells are traversed.

Whenever an intense conductivity is introduced into the medium, the model prompts us to examine the cell matrix size, and to employ appropriately small cells. The small cell size naturally implies larger array sizes, with subsequent complexities in the computer simulations. What are the implications of retaining larger cells, which do not satisfy $R \gg Z_0$? The use of larger cells would of course simplify the computer process. When R is small compared to Z_0 , the wave energy will slosh back and forth in the cell line, changing polarity and decaying with each successive time step. Within the high conductivity region, the solution using a large cell matrix cannot be accurately determined, although it is reassuring that the fields do dissipate after several time steps. So far as the region outside the high conductivity region is concerned, however, the waves may still be obtained with accuracy from the TLM model. The outside waves are repelled from the high conductivity region at the boundary, where the low resistance nodes exist.

The previous comments, concerning the case when $R < Z_0$, will be made more quantitative after we discuss additional aspects of the TLM model. The matter is then taken up in Chapter 7 where we perform simulations in which $R \ll Z_0$ regions exist, and also in App.7A.4 where we discuss the field dissipation in terms of the elementary TLM waves.

1.5 Transmission Line Theory Background

The discussion in the previous sections will be quantified and reconciled with transmission line theory. Before proceeding to this goal, however, we present a brief overview. The literature on transmission line theory is quite extensive (see, e.g., Reference [4]). In this discussion we limit ourselves to only those relationships which are deemed necessary

for describing the technique. Before continuing, it is useful to describe the normal electromagnetic modes in a single section of transmission line, not coupled to any other line elements, in which the terminating resistors are extremely large, i.e., an open circuit. The transmission line is biased to the voltage *difference* V_o and is in an equilibrium state, as shown in Fig.1.10(a). The analysis proceeds by first choosing the correct set of normal modes which describe the standing waves during the off-state, when the line is biased to voltage V_o . This is not difficult to obtain, since we know that the general solution to the wave equation (Eq.(1.2)), or the equivalent Eq.(1.3). Discarding the conductivity term, the solutions are a pair of waves traveling in opposite directions with velocity, v . The simplest set of modes which satisfy the boundary

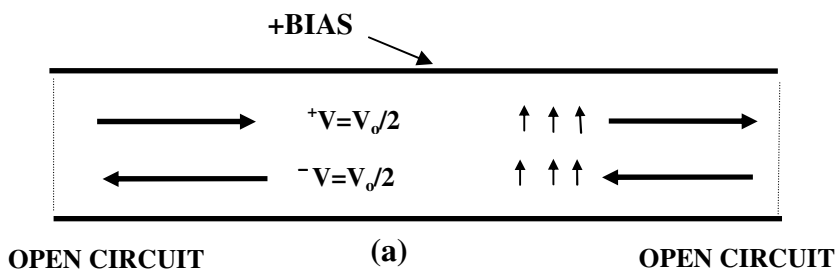


FIG. 1.10(a) STATIC FIELD IN A SINGLE TLM ELEMENT, EXPRESSED IN WAVE VARIABLES. +V AND -V ARE REFLECTED AT ENDS WITH NO CHANGE IN POLARITY OR AMPLITUDE.

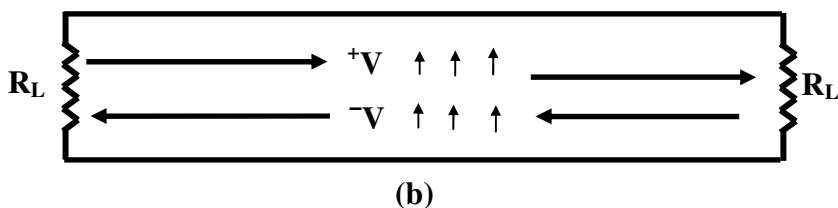


FIG. 1.10(b) TLM CELL IS ACTIVATED AND OPEN CIRCUIT IS REPLACED WITH R_L . LOSS OF AMPLITUDE OCCURS UPON EACH REFLECTION.

conditions, during the off-state, are two waves of the same polarity, each with constant amplitude, and equal to half the bias voltage, $V_0/2$. The two waves travel in opposite directions and are designated ^+V and ^-V in Fig.1.10. ^+V designates the wave traveling in the plus x direction while ^-V is the backward wave traveling in the negative x direction. We adopt the convention that the voltage waves, as indicated by the vertical arrows, point in the direction of increasing voltage (potential). The direction of the electric field is of course opposite to that of the voltage wave. The voltage waves fill the entire transmission element and are constrained by the open circuit at both ends, where the waves are reflected so that ^+V converts to ^-V at one end, and vice versa at the other end. The waves obey the symmetry requirement and of course the waves superimpose to give the correct voltage at all times and at all points in the line during equilibrium, i.e., $V_0 = ^+V + ^-V = ^+(V_0/2) + ^-(V_0/2)$. Thus, the general solution for the voltage consists of a forward wave (positive direction), and a backward wave (negative direction), and the total voltage, which is the equilibrium bias voltage, equal to the sum of the two waves. What happens when we depart from equilibrium, i.e., we allow the open circuit resistance to suddenly decrease in value, as in Fig.1.10(b)? Just as before, there will exist forward and backward waves, but their amplitude will no longer be constant in time. As before the total voltage (which is no longer constant in time), will be the sum of the two waves,

$$V = ^+V + ^-V \quad (1.10)$$

In a similar manner, the associated forward and backward current amplitudes are denoted by ^+I and ^-I , respectively, and the total current is

$$I = ^+I + ^-I \quad (1.11)$$

Next we write down the relationships between the voltage and current waves:

$$^+I = ^+V / Z_0 \quad (1.12)$$

$$^-I = -^-V / Z_0 \quad (1.13)$$

where Z_0 is the characteristic impedance of the line. The minus sign for the backward current wave is significant and is indicative of the fact that the current is moving in the negative direction, away from the load (this is consistent with the opposing magnetic fields associated with the forward and backward voltage waves, ^+V and ^-V). Next, we take note of the

boundary condition which exists at the load. If R_L is the load (assumed to be real) at either junction, then at the load V and I satisfy

$$V = R_L I \quad (1.14)$$

At this point we define two types of voltage coefficients. The reflection coefficient, B , relates the reflected wave ^-V to the incident wave ^+V , while the transfer coefficient, T , relates the load voltage V to the incident wave. Thus,

$$B = ^-V / ^+V \quad (1.15)$$

$$T = R_L I / ^+V \quad (1.16)$$

If Eqs.(1.10)-(1.14) are utilized then these coefficients become

$$B = (R_L - Z_o) / (R_L + Z_o) \quad (1.17)$$

$$T = 2R_L / (R_L + Z_o) \quad (1.18)$$

These coefficients play a pivotal role in the dispersal of the electromagnetic signal due to the conductivity. One should point out that R_L may include not only the terminating resistors, but also the characteristic impedances of any adjoining transmission lines. If an adjoining cell has an impedance, Z_1 , and the junction resistance is R , then the load impedance seen by a wave in Z_o , is the parallel combination given by $R_L = Z_1 R / [R + Z_1]$. Note that when $Z_1 = Z_o$ and $R \sim \infty$ the cell impedances are matched, $T = 1$, $B = 0$, and the wave flows to the adjoining cell unimpeded.

It is natural to ask whether the transfer and reflection coefficients are related, based on energy flow considerations. This conjecture is indeed confirmed by considering the following relationship:

$$(T^2/R_L) + (B^2/Z_o) = 1/Z_o \quad (1.19)$$

Substitution of Eqs.(1.17)-(1.18) into Eq.(1.19) verifies the relationship. Equation (1.19) has a very simple interpretation. If a wave with unit amplitude, propagating in line Z_o , encounters a node with load impedance R_L , then Eq.(1.19) merely states that the incident energy flow, $1/Z_o$, is equal to the energy flow delivered to R_L (i.e., T^2/R_L) plus the energy flow reflected from the load (i.e., B^2/Z_o). Knowing one of the coefficients, however, does not automatically provide us with the other. For example, calculating B from Eq.(1.19) (based on a knowledge of T)

leaves us with an ambiguity as to the sign of B; the original definition of B, Eq.(1.17), must then be used. From Eq.(1.17) we see, therefore, that B is positive when R_L exceeds Z_0 and negative when R_L is less than Z_0 .

In the previous paragraphs we depicted a situation in which a single wave in a transmission line was incident on the load impedance. Now suppose the load is nothing more than another transmission line with a differing impedance, and further suppose the second line also has an signal incident on the node separating the two transmission lines. The situation is illustrated in Fig.1.11 where the two TLM lines are Z_A and Z_B (both very long) and the corresponding incident wave voltages are $+V_A$ and $-V_B$. When we apply the TLM theory to this situation, does our interpretation of results change in any significant manner? We proceed by applying the TLM formulation individually to each of the two incident waves $+V_A$ and $-V_B$. In the case $+V_A$, $R_L=Z_B$, and this produces a transmitted wave $[2Z_B/(Z_A+Z_B)] \cdot +V_A$ and a reflected wave $[(Z_B-Z_A)/Z_A+Z_B] \cdot +V_A$. Likewise, in the case of $-V_B$, the load seen by $-V_B$ is Z_A , and the transmitted and reflected waves are $[2Z_A/(Z_A+Z_B)] \cdot -V_B$ and $[(Z_A-Z_B)/Z_A+Z_B] \cdot -V_B$ respectively. Adding the results (linearly) in each line for both waves one can check out that the continuity of voltage at the node is preserved in the presence of two incident waves. We first obtain the two waves moving away from the node (after interacting with the node). The total backward wave in Z_A will be

$$-V_A^{k+1} = [(Z_B-Z_A)/Z_A+Z_B] \cdot +V_A^k + [2Z_A/(Z_A+Z_B)] \cdot -V_B^k \quad (1.20)$$

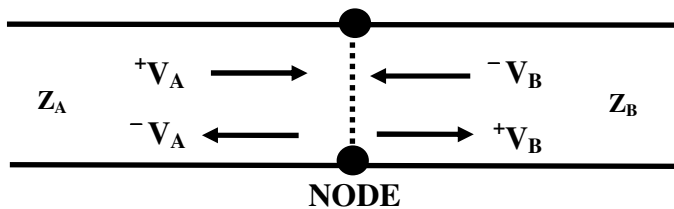


FIG. 1.11 WAVES $+V_A$ AND $-V_B$ INCIDENT ON NODE SEPARATING Z_A AND Z_B . CONTRIBUTIONS TO $-V_A$ AND $+V_B$ (THE REFLECTED AND TRANSMITTED TERMS) ADD LINEARLY.

while the forward wave in Z_B will be

$${}^+V^{k+1}_B = [(Z_A - Z_B)/(Z_A + Z_B)] \cdot {}^-V^k_B + [2Z_B/(Z_A + Z_B)] \cdot {}^+V^k_A \quad (1.21)$$

For the sake of clarity, we have appended $k+1$ and k superscripts (k an integer) in Eqs.(1.20)-(1.21) to denote time step. k and $k+1$ represent the fields before and after scattering respectively. We can then verify that the total voltage at the node is $V = {}^+V_A + {}^-V_A = {}^+V_B + {}^-V_B$. It is worthwhile to make sure that the wave energies carried away from the node, associated with ${}^-V_A$ and ${}^+V_B$, preserve the energy flow. We know that the total energy flow incident on the node, E_T , is given by

$$E_T = (1/Z_A) ({}^+V_A)^2 + (1/Z_B) ({}^-V_B)^2 \quad (1.22)$$

It is then easy to verify that the energy carried away from the node satisfies

$$\begin{aligned} E_T &= (1/Z_A) ({}^+V_A)^2 + (1/Z_B) ({}^-V_B)^2 \\ &= (1/Z_A) ({}^-V_A)^2 + (1/Z_B) ({}^+V_B)^2 \end{aligned} \quad (1.23)$$

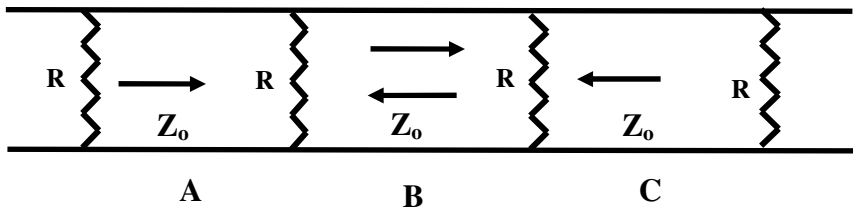
using Eqs.(1.20) and (1.21). We should take care to note the changes in wave direction in Eqs.(1.22) and (1.23). We have not included losses, represented by R at the node. If we do so, then in addition to the wave energies carried away by ${}^-V_A$ and ${}^+V_B$, there will be resistive losses given by V^2/R , but just as before $V = {}^+V_A + {}^-V_A = {}^+V_B + {}^-V_B$.

1.6 Initial Conditions of Special Interest

Before we apply the transmission line concepts and relationships to the iterative methods, we first check the consistency of the model under initial conditions of special interest. Looking at Fig.1.12, we consider the case where Z_A and Z_B are initially biased to the same voltage, V . We assume at that point in time the forward and backward waves in A and B satisfy $V = {}^+V_A + {}^-V_A$ in A and likewise $V = {}^+V_B + {}^-V_B$ in B. All the amplitudes are equal. We now pose the question: during the next time step, will the same static conditions be preserved? The answer is affirmative as may be seen from Eq.(1.20), where on the right hand side, ${}^-V^k_B = {}^+V^k_A$, and thus ${}^-V^{k+1}_B = {}^+V^k_A$ and similarly from Eq.(1.21), ${}^+V^{k+1}_B = {}^-V^k_B$.

Thus the node appears as an open circuit and static conditions are preserved with no net transfer of energy from one line to the other.

Also of much interest is the decay of the various cells for an infinitely long uniform 1D chain in which each cell with the same impedance Z_0 is initially biased to V_0 and each cell contains a node resistance R is finite, as in Fig.1.12. Under these circumstances one may use the relations in Fig.1.12 to determine the decay within each cell. For large R (relative to the line impedance) the forward and backward waves decay by an amount $(1-Z_0/2R)$ with each time step. Because the node resistance and line impedance are uniform, however, we may adopt the view that there is no net transfer of energy from one cell to another. The cell voltage in each cell declines, to be sure, but the decline may be regarded as internal to the cell. The situation changes of course when the adjacent node resistors differ, even when the initial bias voltage is uniform for all the cells. Under these circumstances the fields will redistribute themselves among the cells and a net transfer of energy from one cell to another will occur.



FORWARD WAVE IN B FOR (K+1)TH TIME STEP:

$$+V_B^{k+1} = T^+V_A^K + B^-V_B^k$$

BACKWARD WAVE IN B FOR (K+1)TH TIME STEP:

$$-V_B^{k+1} = T^-V_C^K + B^+V_B^k$$

$$T = 2R_L / (Z_0 + R_L), \quad B = (R_L - Z_0) / (Z_0 + R_L),$$

$$R_L = Z_0 R / (Z_0 + R)$$

FIG. 1.12 WAVES IN A AND C CELLS CONTRIBUTE TO THE FIELD IN B DURING THE ENSUING K+1 TIME STEP ACCORDING TO THE ABOVE RELATIONS. LOSS AND IMPEDANCE IN EACH CELL ARE ASSUMED IDENTICAL.

What happens when the adjoining lines are initially biased to *differing* voltages, even when the node resistors are infinitely large and the cell impedances are uniform? The forward wave going from A to B will not be compensated by the backward wave going from B to A. Equilibrium therefore is not maintained for the one dimensional array. As mentioned before, artificial changes may be introduced, for example, by placing series switches between line elements and activating these switches at the same time that the node resistors is activated. Such changes are not based on any physical considerations, and cannot be seriously considered. The only self consistent solution is to resort to either 2D or 3D arrays, which we do in a later Section of this Chapter. Despite the lack of an initial equilibrium solution (for spatial variations in the voltage), however, the 1D circuit is nevertheless very useful for a host of 1D problems as well as for gaining insight into the more complicated 2D and 3D arrays. In the following we compare the TLM and finite difference methods for obtaining 1D solutions.

One Dimensional TLM Analysis. Comparison with Finite Difference Method

1.7 TLM Iteration Method

We begin the comparison of the 1D TLM and finite difference methods by first considering the TLM iterations. For simplicity we assume the same resistance, R , separating the adjoining lines, which have the same characteristic impedance Z_0 . During a given time interval the sum of the forward and backward waves, ^+V and ^-V , comprise the total field V . As noted previously, the field waves may be written in terms of the fields belonging to the prior interval. Using Fig.1.12 as a guide, the iterative equations for the forward and backward waves in cell B, during the $(k+1)$ th step, are repeated

$$^+V_B^{k+1} = T ^+V_A^k + B^-V_B^k \quad (1.24)$$

$$^-V_B^{k+1} = T ^-V_C^k + B^+V_B^k \quad (1.25)$$

where

$$T = 2R_L / (Z_0 + R_L) \quad (1.26a)$$

$$B = (R_L - Z_0)/(R_L + Z_0) \quad (1.26b)$$

and

$$R_L = Z_0 R / (Z_0 + R) \quad (1.27)$$

The integer superscripts $k, k+1$, attached to the cell fields, denote the time step. The reflection coefficient B should not be confused, of course, with the label of the middle cell. In order to facilitate the comparison with the finite difference method, we introduce the loss parameter,

$$\alpha = Z_0 / 2R \quad (1.28)$$

The scattering coefficients then become

$$T = 1/(1+\alpha) \quad (1.29)$$

$$B = -\alpha/(1+\alpha) \quad (1.30)$$

Adding ${}^+V_B^{k+1}$ and ${}^-V_B^{k+1}$ we obtain the forward iteration for the B cell, or

$$V_B^{k+1} = [(1/(1+\alpha))] [{}^+V_A^k + {}^-V_C^k] - [\alpha/(1+\alpha)] V_B^k \quad (1.31)$$

In order to proceed further with the comparison with numerical methods, we shall need not only the forward iteration, but the “reverse” one as well, for which we shall have to digress.

1.8 Reverse TLM Iteration

Numerical techniques involving partial differential equations often require time elements of $t-\Delta t$ as well as $t+\Delta t$, in order to obtain correct solutions. It should come as no surprise, therefore, that in order to compare the numerical methods with the TLM method, we need to take into account reverse as well as forward iterations. The generic form of the two types of TLM iterations are shown in Eqs.(1.32)-(1.33), applicable not only to 1D but 2D and 3D as well.

FORWARD

$${}^+V^{k+1} = \sum [S.C.] {}^+V^k + \sum [S.C.] {}^-V^k \quad (1.32a)$$

$${}^-V^{k+1} = \sum [S.C.] {}^+V^k + \sum [S.C.] {}^-V^k \quad (1.32b)$$

REVERSE

$${}^+V^{k-1} = \sum [S.C.] {}^+V^k + \sum [S.C.] {}^-V^k \quad (1.33a)$$

$${}^-V^{k-1} = \sum [S.C.] {}^+V^k + \sum [S.C.] {}^-V^k \quad (1.33b)$$

where [S.C.] are the scattering coefficients (evaluated during the k th step) and the summation is over wave contributions from adjacent lines. Note the important fact that in the reverse iteration, the $(k-1)$ th wave is determined from waves existing during the ensuing k th step, whereas the forward iteration relates V^{k+1} to waves existing during the prior k th step. Although Eqs.(1.32) and (1.33) appear to be superficially the same, they are different. First of all, the scattering coefficients will differ, especially if losses are present. In addition, the two iterations will have different node locations for the forward and reverse iterations, which we discuss later.

It seems somewhat strange to consider reverse TLM iterations. One naturally asks the question whether it is truly necessary to examine such a topic. There are at least two reasons, however, why it is important to take into account the reverse iteration. The first is that, using such an iteration, it may be possible to determine an earlier physical state based on the present state. The second reason is that the reverse iteration provides us with additional information, and when we combine both forward and reverse iterations we are able to make a more accurate comparison with other numerical techniques, such as the finite difference technique. In fact we shall see that the finite difference equation may be “decomposed” into forward and reverse TLM iterations, both of which have immediate physical significance.

Although the forward iteration is fairly straightforward, it is not at all clear how one may obtain the reverse type. Table 1.2 provides a prescription, based on a knowledge of the waves during the k th step.

Thus we assume the forward and backward waves, $+V^k$ and $-V^k$, are known in all cells, where the superscript denotes the time step. We then reverse the direction of all the waves; we denote this operation by $*$. Thus $(+V^k)^*$ and $(-V^k)^*$ denotes the wave reversal of $+V^k$ and $-V^k$ during the k th step. We therefore may write the waves which have been reversed as $(+V^k)^* = -V_R^k$ and $(-V^k)^* = +V_R^k$, and we should also take note of the obvious relationships $((+V^k)^*)^* = (-V_R^k)^* = +V^k$, $((-V^k)^*)^* = (+V_R^k)^* = -V^k$. The subscript R is added for clarity in this Section and in Table 1.2, to denote the reversed wave. In the ensuing Sections, however, we will drop the subscript since the reversed waves are always identified as such. The next phase is to calculate the scattering among the reversed TLM waves, treating these waves in the same manner as the usual forward iteration. We then proceed to calculate the waves for the next step, but with an important difference. During the scattering any node resistors are considered negative, i.e., the signals are amplified. This is to be expected, since we are going back in time and any attenuated signals must regain their former strength by being amplified.

TABLE 1.2
HOW TO GO BACK IN TIME VIA THE REVERSED
TLM ITERATION

- 1) **ASSUME WAVE $+V^k$ AND $-V^k$ ARE KNOWN (FOR THE FORWARD ITERATION)**
- 2) **REVERSE DIRECTION OF ALL WAVES $(+V^k)^* \rightarrow -V_R^k$, $(-V^k)^* \rightarrow +V_R^k$**
- 3) **AS IN FORWARD ITERATION, CALCULATE THE WAVE SCATTERING AND OBTAIN $+V_R^{k+1}$ AND $-V_R^{k+1}$. TIME DEPENDENT NODES ARE EVALUATED AT THE k TH STEP**
- 4) **DURING SCATTERING, ANY NODE RESISTORS ARE CONSIDERED NEGATIVE, I.E., SIGNALS ARE AMPLIFIED**
- 5) **UPON COMPLETION OF SCATTERING, REVERT TO ORIGINAL DIRECTION, $(+V_R^{k+1})^* \rightarrow -V^{k-1}$, $(-V_R^{k+1})^* \rightarrow +V^{k-1}$**

We should also note that the nodes used in the scattering are evaluated at the same k th time step (with negative node resistance). The final step, after the completion of the scattering, is to revert to the original directions of the waves, or $({}^+V_R^{k+1})^* \rightarrow {}^-V^{k-1}$ and ${}^-V_R^{k+1} \rightarrow {}^+V^{k-1}$.

Suppose we have knowledge of the present and future TLM fields and nodes, but are ignorant of any prior states. Is it possible to obtain a similar knowledge of the previous states? The reversion to an earlier state, by means of the reversed iteration, is certainly achievable provided the nodes are time independent. With time independent nodes we presumably have a knowledge of the nodes throughout the medium at all times and therefore we can go back in time as far wish.

With time *dependent* nodes, however, there is in general no way to determine the prior states, even when the node resistance is much larger than the line impedance. In order to attempt such an effort we must first resort to an examination of the fields and nodes, as well as the time and spatial gradients of the fields and nodes, during the present and future states. With such information it is conceivable we can make educated “guesses” as to the prior states. Certainly the first few states just prior to the present state may be estimated by analytically continuing the node values back in time. Also, if we somehow know (or guess) the static field configurations of the initial state existed in a given, limited region, then this information may possibly provide clues as to such prior states (in this case the unknown prior states occur after activation). Further scrutiny of this topic, as well as questions concerning the uniqueness of the solution, will take us far beyond the scope of the present discussion.

Although we have considered adjacent cells to have the same impedance, Z_0 , the procedure for finding V^{k-1} is exactly the same when the cell impedances differ. A simple example may be provided by a linear chain (1D) of cells having the same dielectric constant but differing impedance values. Suppose at some point in time, say, the k th time step, the fields are zero in all the cells except for adjoining cells A and B (position-wise, cell B is positive with respect to A). The impedance values of cells A and B are assumed to be Z_0 and $2Z_0$, respectively. Now suppose that during the k th time step in cells A and B we find the fields are ${}^-(1/3)_A^k$ and ${}^+(4/3)_B^k$ respectively (and zero in the other cells). How do we obtain the fields in the $(k-1)$ th time step? We simply reverse the directions of the fields (so the fields become ${}^+(1/3)_A^k$ and ${}^-(4/3)_B^k$) and thence allow the iteration to proceed to the $(k+1)$ th time

step. The result is ${}^{-}(1)_A^{k+1}$. Reversing this wave, and replacing $k+1$ with $k-1$, then results in ${}^{+}(1)_A^{k-1}$. The reader may confirm the result by proceeding with the forward iteration, starting with $(k-1)$ th time step.

1.9 Derivation of Scattering Coefficients for Reverse Iteration

We now return to the case where loss is included at the nodes. In our prescription for finding V^{k-1} , we said that we replace R with $-R$ in the scattering coefficients, or, alternatively, α with $-\alpha$. We now verify this assumption. Figure 1.13 shows the status of the waves during the $(k-1)$ th step where V^{k-1}_1 and V^{k-1}_2 are the waves in cells 1 and 2 respectively and the coefficients T and B are given by Eqs.(1.29) and (1.30). During the k th time step the backward wave in cell 1 is

$${}^{-}V_1^k = (-\alpha^+V_1^{k-1} + {}^{-}V_2^{k-1})/(1+\alpha) \tag{1.34}$$

and the reversed wave is

$$({}^{-}V_1^k)^* = {}^{+}V_1^k = (-\alpha^+V_1^{k-1} + {}^{-}V_2^{k-1})^*/(1+\alpha) \tag{1.35}$$

Similarly the forward field in the second cell is

$${}^{+}V_2^k = ({}^{+}V_1^{k-1} - \alpha{}^{-}V_2^{k-1})/(1+\alpha) \tag{1.36}$$

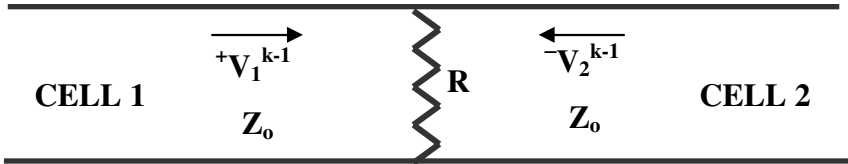
After reversal this wave becomes

$$({}^{+}V_2^k)^* = {}^{-}V_2^k = ({}^{+}V_1^{k-1} - \alpha{}^{-}V_2^{k-1})^*/(1+\alpha) \tag{1.37}$$

We then use the reversed fields, ${}^{+}V_1^k$ and ${}^{-}V_2^k$, and proceed to the next (reverse) step, using the usual iterative Eqs.(1.24) and (1.25) (with as yet unknown scattering coefficients) to obtain ${}^{-}V_1^{k+1}$ and ${}^{+}V_2^{k+1}$. We then perform a final reversal, and ${}^{-}V_1^{k+1}$ and ${}^{+}V_2^{k+1}$ become ${}^{+}V_1^{k-1}$ and ${}^{-}V_2^{k-1}$. The final equations are

$$\begin{aligned} {}^{+}V_1^{k-1} &= [(-\alpha^+V_1^{k-1} + {}^{-}V_2^{k-1})/(1+\alpha)] B_G \\ &+ [({}^{+}V_1^{k-1} - \alpha{}^{-}V_2^{k-1})/(1+\alpha)] T_G \end{aligned} \tag{1.38}$$

$$\begin{aligned} {}^{-}V_2^{k-1} &= [(-\alpha^+V_1^{k-1} + {}^{-}V_2^{k-1})/(1+\alpha)] T_G \\ &+ [({}^{+}V_1^{k-1} - \alpha{}^{-}V_2^{k-1})/(1+\alpha)] B_G \end{aligned} \tag{1.39}$$



SCATTERING COEFFICIENTS: $T = 1/(1+\alpha)$, $B = -\alpha/(1+\alpha)$, $\alpha = Z_0/2R$

FIRST CELL, Kth STEP: $-V_1^k = (-\alpha +V_1^{k-1} + -V_2^{k-1})/(1+\alpha)$

REVERSED WAVE $=(-V_1^k)^* = +V_1^k = (-\alpha +V_1^{k-1} + -V_2^{k-1})^*/(1+\alpha)$

SECOND CELL, KTH STEP: $+V_2^k = (+V_1^{k-1} - \alpha -V_2^{k-1})/(1+\alpha)$

REVERSED WAVE $= (+V_2^k)^* = -V_2^k = \{+V_1^{k-1} - \alpha -V_2^{k-1}\}^*/(1+\alpha)$

PROCEEDING TO THE NEXT(REVERSED) STEP, $-V_1^{k+1}$, $+V_2^{k+1}$ ARE OBTAINED. A FINAL REVERSAL IS THEN DONE TO RETRIEVE $+V_1^{k-1}$ AND $-V_2^{k-1}$ EQS.(1.38)-(1.39) AND REVERSE S.C., T_G, B_G .

FIG. 1.13 DETERMINATION OF REVERSE COEFFICIENTS. ABOVE IS STATUS DURING (k-1)TH STEP. PRESCRIPTION IN TABLE 1.2 IS FOLLOWED TO OBTAIN THE REVERSE COEFFICIENTS, T_G, B_G .

In Eqs.(1.38)-(1.39), T_G, B_G are the as yet unknown coefficients which allow us to regain $+V_1^{k-1}$ and $-V_2^{k-1}$. Solving for these coefficients gives us

$$T_G = 1/(1-\alpha) \tag{1.40a}$$

$$B_G = \alpha/(1-\alpha) \tag{1.40b}$$

Both Eqs.(1.38) and (1.39) yield the same expressions for T_G and B_G , as required for consistency. Note that T_G and B_G are identical to Eqs.(1.29)-(1.30) when we substitute $-\alpha$ for α , i.e., $-R$ for R . As promised the reverse iterations require that we substitute negative values for the node resistance in the scattering coefficients. This will enable us to perform the reverse iteration we need to complement the forward iteration in Eq.(1.31).

It is a curious fact that to a certain degree we possess the mathematical tools (certainly for time independent nodes) to go back in time, as well as forward. The reverse iteration may be used to view earlier events, based on present events. Does a preference exist for one or the other process, based on experience? Based on observation, the answer is yes. Nature appears to favor the forward direction; in the present context this corresponds to the tendency of electromagnetic energy to spread out in the available spatial directions.

1.10 Complete TLM Iteration (Combining Forward and Reverse Iterations)

Having verified the scattering coefficients for the reverse wave, Eqs. (1.40a)-(1.40b), we can obtain the reverse iteration, which will enable us to determine the complete TLM equation. Using the designations in Fig.1.12, we now must now focus on $^-V_A^k$ and $^+V_C^k$ (instead of $^+V_A^k$ and $^-V_C^k$) in cells A and C. We then resort to the our oft-stated method, and reverse the direction of waves $^-V_A^k$ and $^+V_C^k$, allow the iteration to proceed for one step, using Eqs.(1.40a)-(1.40b), and finally revert to the original direction. The reverse iteration for cell B is then

$$V_B^{k-1} = [(1/(1-\alpha)] [^-V_A^k + ^+V_C^k] + [\alpha/(1-\alpha)] V_B^k \quad (1.41)$$

If we compare the above with V_B^{k+1} , Eq.(1.31), we see that a shortcut method for obtaining V_B^{k-1} exists: In Eq.(1.31) we simply replace α with $-\alpha$ and also replace any forward wave with a backward wave, and similarly any backward wave with a forward one. For purposes of comparison with numerical methods, we add V_B^{k-1} and V_B^{k+1} obtaining

$$V_B^{k+1} + V_B^{k-1} = [(V_A^k + V_C^k) + \alpha(-^+V_A^k - ^-V_C^k + ^-V_A^k + ^+V_C^k) + 2\alpha^2 V_B^k]/(1-\alpha^2) \quad (1.42)$$

We will see shortly that the above is compatible with the iteration obtained by finite difference methods. We thus may regard the finite difference iteration as a combination of forward and backward TLM iterations.

1.11 Finite Difference Method. Comparison with TLM Method

We now turn to the conventional numerical technique for solving the wave equation, which relies on the use of finite differences (see, e.g., Reference [5]). A rectangular grid for the distance x and time t coordinates is first established. We then perform a Taylor expansion of the second order spatial derivative of $E(x,t)$ about x , and evaluated at two locations: $x-\Delta x$ and $x+\Delta x$, where Δx represents a small excursion from x . The results for the two locations are subtracted,

$$\begin{aligned} \partial^2 E(x,t)/\partial x^2 = [E(x + \Delta x,t) - 2E(x,t) + E(x - \Delta x,t)]/\Delta x^2 \\ + \text{higher order terms} \end{aligned} \quad (1.43)$$

where Δx is the difference in the x coordinate. Similar expansions of $\partial^2 E(x,t)/\partial t^2$ and $\partial E(x,t)/\partial t$ yield

$$\begin{aligned} \partial^2 E(x,t)/\partial t^2 = [E(x,t + \Delta t) - 2E(x,t) + E(x,t-\Delta t)]/\Delta t^2 \\ + \text{higher order terms} \end{aligned} \quad (1.44)$$

$$\begin{aligned} \partial E(x,t)/\partial t = [E(x, t + \Delta t) - E(x, t - \Delta t)]/2 \Delta t \\ + \text{higher order terms} \end{aligned} \quad (1.45)$$

where Δt is the difference in the time. Substituting Eqs.(1.43)-(1.45) into the wave equation and solving for $E(x,y,t+\Delta t)$ yields the iterative equation,

$$\begin{aligned} E(x,t + \Delta t) = E(x,t) - E(x, t - \Delta t) + \lambda^2 [E(x + \Delta x,t) + E(x-\Delta x, t) - 2E(x,t)] \\ - \alpha [E(x,t + \Delta t) - E(x,t - \Delta t)] \end{aligned} \quad (1.46)$$

$$\text{where} \quad \lambda^2 = v^2 \Delta t^2 / \Delta x^2 \quad (1.47a)$$

$$\alpha = \Delta t \sigma / 2 \quad (1.47b)$$

Eq.(1.46) simplifies by setting $\lambda=1$, or $\Delta x=v\Delta t$. The value for λ is within the allowable range needed to insure stability for the finite difference solution. Stability is assured when the “numerical” velocity, $\Delta x/\Delta t$, is greater than or *equal* to the wave velocity v (Reference [5]). Since $\Delta x/\Delta t$

is set equal to v , the finite difference solution is automatically stable and Eq.(1.46) becomes

$$E(x,t + \Delta t) = - E(x, t - \Delta t) + [E(x + \Delta x,t) + E(x - \Delta x, t)] - \alpha[E(x,t + \Delta t) - E(x,t-\Delta t)] \quad (1.48)$$

In order to compare the above with the TLM iteration we convert the field variables to TLM variables, setting Δx equal to Δl , and using the following correspondence:

$$E(x,t) \rightarrow V_B^k \quad E(x,t + \Delta t) \rightarrow V_B^{k+1}, \quad E(x - \Delta x, t) \rightarrow V_A^k, \text{ etc.} \quad (1.49)$$

The finite difference equation then becomes

$$V_B^{k+1} + V_B^{k-1} = V_A^k + V_C^k - \alpha[V_B^{k+1} - V_B^{k-1}] \quad (1.50)$$

Substitution of the TLM iterations for V_B^{k+1} , V_B^{k-1} , Eqs.(1.31), (1.41), into the above then *yields an identity*. The TLM and finite difference iterations are therefore completely compatible. We should add, that from a mathematical point of view, there are innumerable combinations of V_B^{k+1} and V_B^{k-1} which satisfy Eq.(1.50). Equations (1.31) and (1.41), however, are the only ones which satisfy the physical requirements imposed by the motion of the forward and backward TLM waves. We assert, therefore, that we can break up the 3 tier finite difference iteration into a pair of two tier forward and reverse iterations, corresponding to the motions of forward and reverse TLM waves, and given by Eqs.(1.31) and (1.41). As a practical matter, of course, the forward iteration is most often used, although the reverse iteration may on occasion be invoked.

2D TLM Analysis. Comparison with Finite Difference Method

The transition from 1D to 2D exposes the potential advantages and flaws of the transmission line matrix method. One advantage, alluded to before, is that the 2D matrix allows for static solutions without the artificial insertion of any components (such as a switch). There is therefore a smooth passage from the static solution to the transient one, once the equilibrium conditions are upset. Another advantage has to do with the fact that the transmission lines border a symmetry element, in this case a square (or in 3D, a cube). The symmetry elements occupy the entire space, which of course is essential, and in addition the elements can be

labeled in a natural way. The notation used for these elements is discussed in Chapter 2.

One shortcoming of the 2D (and 3D) matrices, which is repairable, stems from the lack of isotropy when using symmetry elements. Thus when using a 2D TLM matrix the electromagnetic energy is constrained to move along the lines surrounding the square element. As a result, if a signal source emanates from the source region O, the *first arrival time* of a signal reaching point B will exceed that for point B, as shown in Fig.1.14. This is because the path OA is a straight line while that of OB must proceed along a zigzag path. In an isotropic medium there is no reason why these two directions should differ. This effect is not surprising since the square element (or any other symmetry element, for that matter) is not isotropic. This and other related topics are discussed in Chapters 2-4, where we also modify the technique to compensate for the inherent anisotropy of the square symmetry element. One should also note that as the cell size is further diminished, the width of the earliest arriving signal will likewise diminish and eventually disappear.

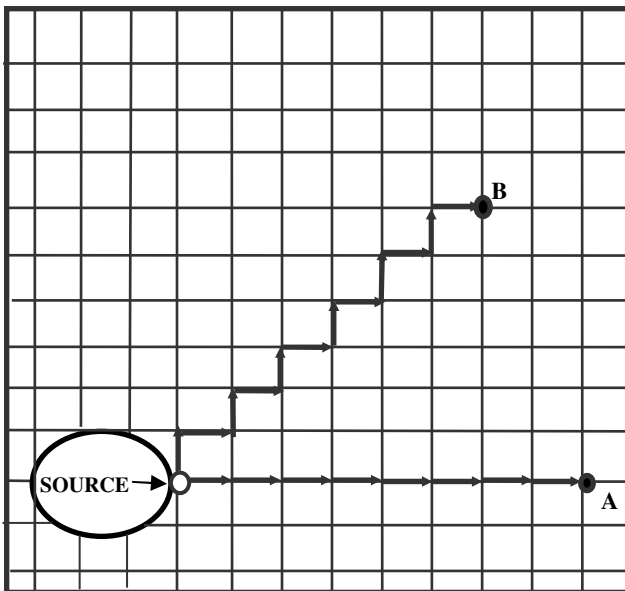


FIG. 1.14 DIRECTIONAL ANISOTROPY OF SQUARE MATRIX.

A second shortcoming has to do with the fact that the 2D and 3D matrices do not possess plane wave properties. We correct the cell matrix, so as to account for plane wave effects, in Chapter 4.

Despite the aforementioned limitations, we will show that the two dimensional matrix of transmission lines is closely linked with the finite difference solutions of the two dimensional wave equation. For the treatment of the two dimensional problem, we compare a two dimensional matrix of transmission lines with the two component wave equations in the x and y directions. In the following discussion, the 2D comparison of the finite difference and TLM methods does not include losses, but this does not alter the generality of the conclusions in any way. The ensuing Chapters of course include loss terms in the TLM iterations. We begin with the transmission line discretization, first discussing boundary conditions at the node, followed by the static and non-static behavior.

1.12 Boundary Conditions at 2D Node

In the ensuing Sections we will assume the time step to be small enough so that the fields change very little during the step. In addition, the fields at the node are considered to be irrotational. As we shall see later, the rotational properties come into play once the scattering to the lines about the node occurs.

Figure 1.15 shows the node of a 2D array. If we look at line A, e.g., we see that it is coupled to three other transmission lines. The isotopotential regions, which form the boundaries of the four lines emanating from the node, are denoted by V_1, V_2, V_3 , and V_4 . The voltage *difference* in the line separating cells 1 and 2 is $V_A = V_2 - V_1$, with similar relations for the other lines. The complete set is:

$$V_A = V_2 - V_1 \quad (1.51a)$$

$$V_B = V_4 - V_3, \quad (1.51b)$$

$$V_C = V_3 - V_1, \quad (1.51c)$$

$$V_D = V_4 - V_2. \quad (1.51d)$$

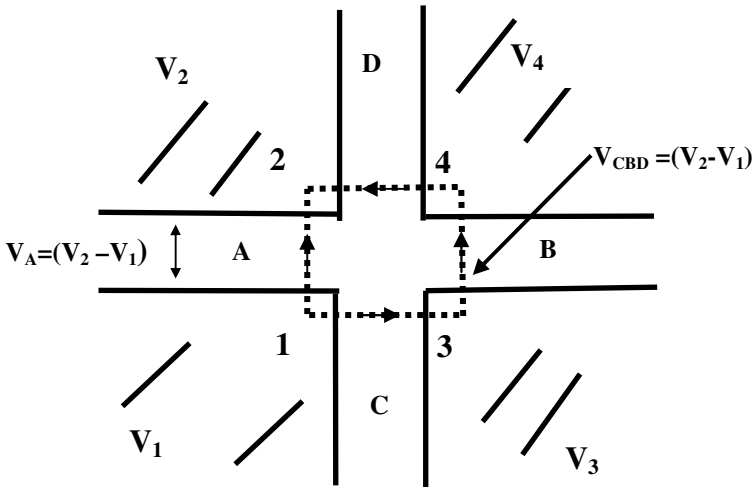


FIG. 1.15. BOUNDARY CONDITION AT 2D NODE
IS $V_A = V_C + V_B - V_D$, WHERE $V_A = V_{CBD} = V_2 - V_1$,
 $V_B = V_4 - V_3$, $V_D = V_4 - V_2$.

Since we assume the node region is small compared to the wavelengths being generated, we consider the field to be conservative about the node. Thus, the voltage path from 1 to 2 is equivalent to 1 to 3 followed by 3 to 4 and then 4 to 2. We therefore take as our boundary condition

$$V_A = V_B + V_C - V_D \tag{1.52a}$$

It is important to note that the line voltages in the above represent the total voltage, i.e., the sum of the backward and forward voltage waves. Also note the negative sign for V_D , which stems from the fact that the path displacement is in the negative direction. and therefore the voltage wave is negative. The negative sign for V_D is completely dependent on the fact that we have selected V_A as our initial wave, dictating that the other three waves match V_A . We could just as well have selected 1 to 3, 3 to 4, or 2 to 4 in which case the corresponding relations would be

$$V_C = V_A + V_D - V_B \tag{1.52b}$$

$$V_B = -V_C + V_A + V_D \tag{1.52c}$$

$$V_D = +V_B + V_C - V_A \quad (1.52d)$$

Again note that the negative signs indicate a path displacement in either the negative x or y directions. We hope that further confusion is not introduced, concerning sign conventions, if we also remind ourselves that the voltage difference variable is always opposite in sign to the electric field, so for example, $V_A = V_2 - V_1 = \Delta V = -E\Delta l$.

To justify the replacement of the field theory with the transmission line matrix, for both the static and non-static cases, we assume that in the *region of the node*, both electric and magnetic fields, as well as the time, are slowly varying (compared to the TLM element Δl and the time step Δt), so that *on the average*, the fields are irrotational. This implies that the two line integral paths from point 1 to point 2, as shown in the Figure, are identical. In the case of the electric field, therefore, the fields are assumed to be concentrated in the TLM lines, and we replace the field variables with the line voltages. One should stress that the fields within the transmission lines themselves are rotational, as they must be in order to propagate as a wave. The other boundary condition at the node has to do with the magnetic vector associated with the electric field. The magnetic fields of the lines are all perpendicular to the electric fields, and thus the magnetic fields are perpendicular to the paper. As a boundary condition we insist that the magnetic field be continuous at the junction. Thus, for example, in line A the magnetic field will be equal to magnetic field in each of the lines B, C, and D. In terms of transmission line variables, of course, the magnetic field translates into a line current, and the boundary condition requires continuity of current at the node. The total current in each line, therefore, is identical. The above node boundary conditions are applicable to either static or non-static problems, and the boundary conditions remain the same whether the node resistors are activated or not. The curl properties are automatically satisfied, as will be described in a later Section. In addition, there is no constraint on the values of the characteristic impedances of the lines surrounding the node.

1.13 Static Behavior about 2D Node

The static behavior of the 2D array may be examined, once again using Fig.1.15 We assume the end resistors are much larger than the characteristic impedances, and therefore do not interfere with the assumed static conditions. The approach adapted is suggested by the 1D TLM line seg-

ment, where we know that a single isolated cell at voltage V contains forward and backward waves each with amplitude $V/2$. We determine whether such an arrangement in each of the 2D line segments is self consistent, and remains the same once the waves in each line are allowed to couple to other lines. To explore this, we look at line A. Initially, the forward wave amplitude is ${}^+V_A = (V_2 - V_1)/2$ and it sees a load impedance of $(Z_B + Z_C + Z_D)$. The backward in A, ${}^-V_A$, consists of two parts. First there is the contribution caused by the reflection at the node, denoted by ${}^-V_{A,R}$, and is given by

$${}^-V_{A,R} = [(V_2 - V_1)/2][Z_B + Z_C + Z_D - Z_A] / [Z_A + Z_B + Z_C + Z_D] \quad (1.53)$$

Next we consider the waves in B, C, and D headed in the direction of the node. and ask what part these waves are transferred to line A. Although one can consider each line individually, it is easiest to consider B, C and D as forming a composite line with impedance $(Z_B + Z_C + Z_D)$. The voltage transferred from this composite line into A, denoted by ${}^-V_{BCD}$, is

$${}^-V_{BCD} = (V_2 - V_1) Z_A / [Z_B + Z_C + Z_D + Z_A] \quad (1.54)$$

If we add Eqs.(1.53) and (1.54) then we obtain the total backward wave in A,

$${}^-V_A = {}^-V_{A,R} + {}^-V_{BCD} = (V_2 - V_1)/2 \quad (1.55)$$

But this is simply the reflected wave one would expect from an open circuit. The same result is obtained if we consider the voltage transfer contributions from each of the individual lines, B, C, and D. Similarly, the results are the identical if we consider the other nodes and TLM lines. Thus the initial fields remain constant, i.e., the solution remain stable so long as the resistors are not activated. Unlike the one dimensional matrix, therefore, adjoining cells with differing voltage will remain at the same voltage without discharging into one another.

1.14 Non-static Example: Wave Incident on 2D node

Before deriving the iterative equations for the transmission line matrix, we consider a simple non-static case of a solitary forward wave incident on a 2D node, as in Fig.1.16. As we have mentioned before, the same

boundary conditions and scattering equations apply to the transient situation.

The boundary conditions are further illustrated by supposing that a wave $+V_A$ is launched in line A, directed toward the node. Upon reaching the node, the field description dictates the conservation of voltage at the node. If V_A is the voltage associated with the A line, and likewise V_B, V_C, V_D , are the node voltages in the other lines, then at the node we expect the following to be satisfied during the time step *following* the arrival of $+V_A$ at the node.

$$V_A = +V_A + -V_A \tag{1.56a}$$

$$V_A = V_B + V_C - V_D \tag{1.56b}$$

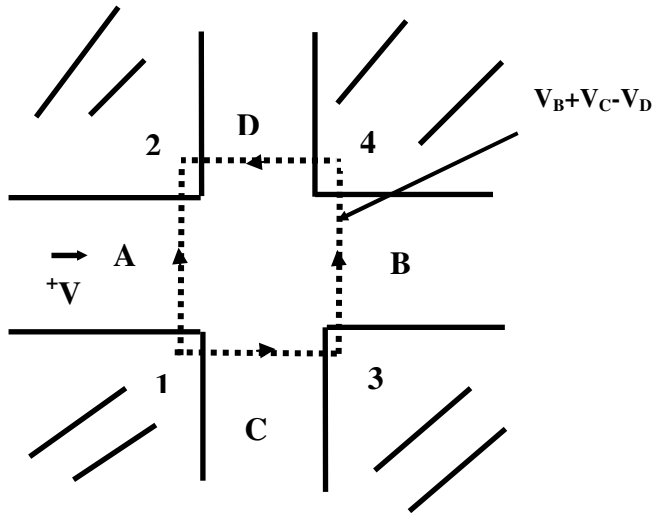


FIG. 1.16 EXAMPLE OF NON-STATIC BEHAVIOR. FORWARD WAVE $+V_A$ IS LAUNCHED IN A, DIRECTED TOWARD NODE. $V_A = +V_A - V_A = V_B + V_C - V_D$ WHEN WAVE REACHES NODE.

Next, we determine how the wave scatters among the various lines. Although transmission line theory automatically satisfies the requirement of voltage conservation at the nodes, it is instructive to verify this

property, i.e., Eq.(1.56), taking into account both reflections and energy transfers into adjoining lines. To simplify matters we assume the lines all have the same impedance, Z_0 . Starting with the reflected wave, since $R_L = 3Z_0$,

$$B = (R_L - Z_0)/(R_L + Z_0) = 1/2 \quad (1.57)$$

and thus

$$^-V_A = B^+V_A = (1/2)^+V_A \quad (1.58)$$

Eqs.(1.57)-(1.58) allow us to calculate the total load voltage V . Thus the sum of the reflected and incident waves is

$$V_A = ^+V_A + ^-V_A = (3/2)^+V_A \quad (1.59)$$

The wave transmitted from A to B, for example, is calculated from

$$^+V_B = T^+V_A \quad (1.60)$$

T may be obtained from

$$T = [2R_L/(R_L + Z_0)] (Z_0/R_L) = 1/2 \quad (1.61)$$

where the (Z_0/R_L) is appended to T since the voltage transfer to B represents only a portion of the voltage delivered to R_L . Combining,

$$^+V_B = (1/2)^+V_A \quad (1.62a)$$

We should note that $^+V_B = V_B$ (the total field) since there is as yet no backward wave in B. Similarly, the voltage transfer to lines C and D are

$$^-V_C = (1/2)^+V_A \quad 1.62b$$

$$^+V_D = -(1/2)^+V_A \quad (1.62c)$$

Again we should note that ^-V_C and ^+V_D represent the total fields V_C , V_D in lines C and D. We should also note the minus sign in Eq.(1.62c), since ^+V_D is directed in the negative x direction. The previous equations are in agreement with the boundary condition, Eq.(1.56b), as expected, i.e., the total field in lines B, C, D is then $(3/2)V$. Although we have considered

a solitary wave in only one of the lines, the situation does not fundamentally change when waves from the other lines (C, B, or D) are simultaneously incident on the node. Under these circumstances the waves moving away from the node, in each line, will not only consist of the reflected wave, but will receive contributions from the incident waves in the other lines, which add in linear fashion to the reflected wave, just as in the 1D case.

In the previous discussion, we focused on a single wave launched in one of the lines. The behavior of the 2D nodes when multiple coherent waves exist in parallel lines, however, is an important issue. Referring to Fig.1.17, we inquire whether identical waves, launched simultaneously in lines R, S, T, etc., will ultimately simulate a plane wave. In other words, we ask whether the waves in R, S, T, transfer completely intact to lines D, E, F, without transverse scattering or reflection. In Chapters 3 and 4 we examine in detail the question of plane waves in 2D and 3D TLM matrices and describe the modifications which must be made to the TLM theory.

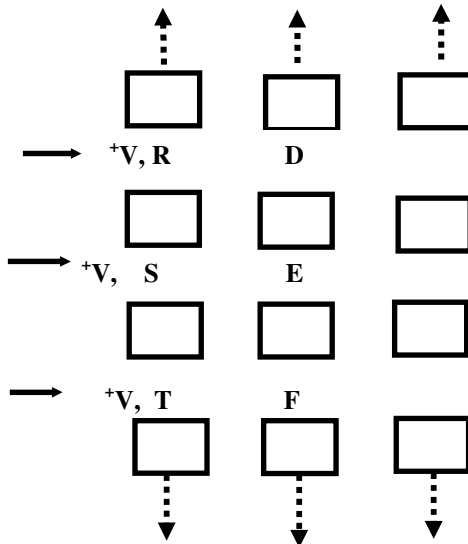


FIG. 1.17 PLANE WAVE SIMULATION WITH IDENTICAL FORWARD WAVES, +V. UNDER PLANE WAVE CONDITIONS, +V IS TRANSFERRED INTACT FROM LINE R TO LINE D, S TO E, ETC...

1.15 Integral Rotational Properties of Field about the Node

Although we rely on the rotational properties of the field within the TLM lines, the fields at the node are considered irrotational. We should therefore be concerned as to whether the fields about the node reflect the necessary rotational properties as expressed in Maxwell's Equations. In order to examine such compatibility we utilize the integral representations of the curl equations. To account for the curl properties, we will have to jump ahead slightly and allow, in a simplified way, for 3D scattering. Chapters 3 and 4 describe the 3D scattering in detail

The rotational boundary conditions at the node are addressed by first considering the curl equation for the magnetic field

$$\nabla \times \mathbf{H} = \mathbf{j} + \partial \mathbf{D} / \partial t \quad (1.63)$$

where the two contributors to the magnetic field are the conduction current density \mathbf{j} and the displacement current $\partial \mathbf{D} / \partial t$ where $\mathbf{D} = \epsilon \mathbf{E}$. We first show that the TLM boundary conditions at the node are consistent with the above curl equation when only conduction current sources are present. We begin with Fig.1.18(a) where an element of current density flow \mathbf{J} is activated via the node resistance, thereby launching waves in lines A and B. Note that \mathbf{J} flowing in the node is assumed orthogonal to the TLM lines, which convey the current.

As a result of the differing forward and backward waves in A and B, a net current wave will flow in these lines, proportional to the *difference* between the voltage wave moving *toward* the node, and the wave moving *away* from the node. In line A this net current is equal to $(+V_A - -V_A)/Z_0$ and in line B it is $(-V_B - +V_B)/Z_0$. A magnetic field is associated with the net current in each line. If the incident voltage waves exceed the voltage wave amplitudes moving away from the node then the magnetic field is pointed into the paper in line A and emerges from the paper in line B.

A more quantitative grasp of the situation may be obtained if we use the integral formulation of the curl equation, which for the conduction current is

$$\int \mathbf{H} \cdot d\mathbf{l} = \int \mathbf{j} \cdot d\mathbf{s} \quad (1.64)$$

where $d\mathbf{l}$ and $d\mathbf{s}$ are the usual line and area differentials. Consider for example all the elements of \mathbf{j} in the x direction, with the line integral in

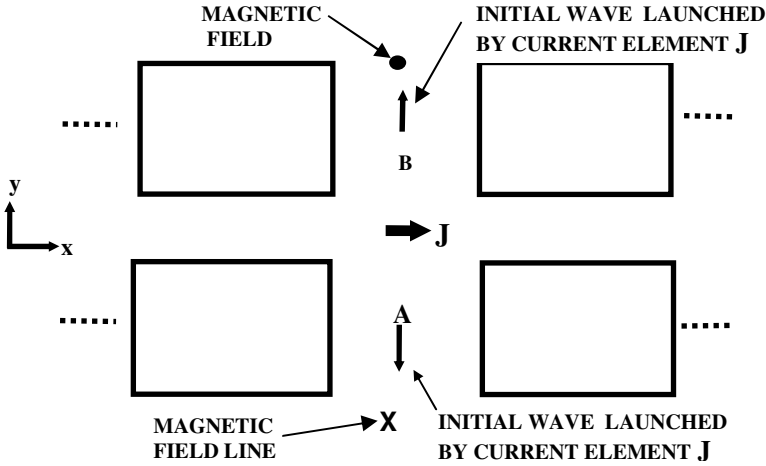


FIG. 1.18(a) GENERATION OF CURLED MAGNETIC FIELD (YZ PLANE) ABOUT NODE IN THE TLM MATRIX, IN RESPONSE TO CURRENT ELEMENT J.

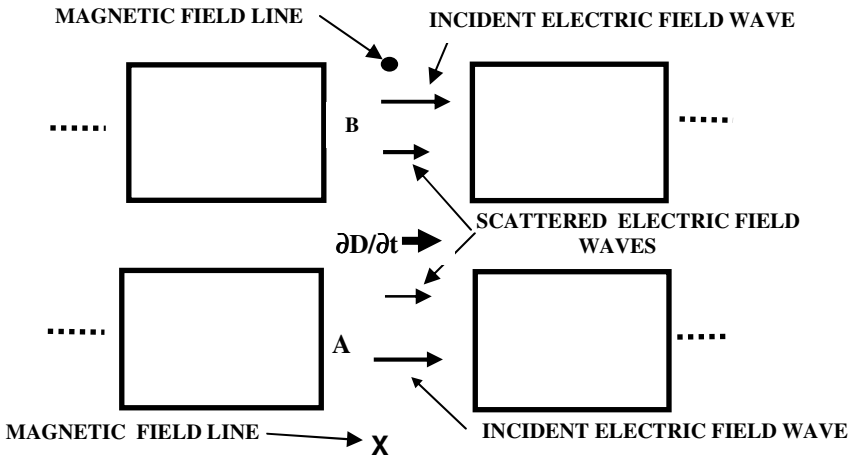


FIG. 1.18(b) GENERATION OF CURLED MAGNETIC FIELD (YZ PLANE) ABOUT NODE IN THE TLM MATRIX, IN RESPONSE TO DISPLACEMENT CURRENT

the yz plane. We can think of the curl equation as representing four separate contributions, one for each TLM line converging at the node with the node current branches in the x direction; these include lines A, B, and the two lines *perpendicular* to the paper. The contribution of each line to the integral about the x axis is expressed in general form as

$$I = (V_1 - V_2)/Z_0 = H\Delta l \quad (1.65)$$

where V_1 is the wave incident on the node and V_2 is the wave moving away from the node (e.g., in line A, $V_1 = +V_A$ and $V_2 = -V_A$). Δl is the elementary line element, and H is the magnetic field associated with each of the four TLM lines surrounding the node in the yz plane. Naturally, each of the four lines need not have the same field, in which case each line will make a different contribution to the integral.

We verify the consistency of the TLM formulation with Eq.(1.64) by first selecting the surface element and the corresponding line integral path in the yz plane, which is dictated by the assumed extent of the fields, Δl . The selection is the element Δl^2 , centered about the node (located at the origin). Assuming identical lines about the node, the yz path selected is $(y - \Delta l/2, z - \Delta l/2) \rightarrow (y + \Delta l/2, z - \Delta l/2) \rightarrow (y + \Delta l/2, z + \Delta l/2) \rightarrow (y - \Delta l/2, z + \Delta l/2)$. The integral on the left side of Eq.(1.64) is then given by $[H(y, z - \Delta l/2) + H(y + \Delta l/2, z) + H(y, z + \Delta l/2) + H(y - \Delta l/2, z)]\Delta l$. Next we look at the area integral for the conduction current given by the right side of Eq.(1.64). The contribution of the net current in each line is given by Eq.(1.65); substitution for each of the four lines then yields an identity, thus verifying the consistency of the curl formulation with the TLM formulation (at least for the conduction current).

It should be noted, of course, that Eq.(1.64) has been verified for only a single cell surrounding the current element. Equation (1.64) must be confirmed throughout the entire propagation space. In addition we must demonstrate that the TLM solution settles down to the correct static solution given by Eq.(1.64). For example the TLM solution should replicate the simple $(1/r)$ dependence of the magnetic field for a straight and infinitely long current carrying wire, where r is the normal distance from the wire to the field point. To do this a 3D treatment with the proper scattering coefficients is essential. In Sections 3.4-3.5, 3.A1. and the simulation in Section 7.20 we outline how the TLM method may be used to approximate static solutions to Eq.(1.64).

The same type of analysis can also be applied to the displacement current as indicated in Fig.1.18(b). The integral representation of the curl equation with displacement current sources is

$$\int \mathbf{H} \cdot d\mathbf{l} = \int \partial (\epsilon \mathbf{E}) / \partial t \cdot d\mathbf{s} \tag{1.66}$$

As before suppose we consider the displacement current sources in the x direction with the line integral in the yz plane. We associate the time change in the displacement field with the advancing wave (either forward or backward) in the TLM line.

When the forward and backward waves have the same polarity and amplitude, the contributions to the magnetic field cancel and electrostatic conditions prevail. When the polarities are opposite the magnetic conditions prevail while the total electric field vanishes. In order to provide additional generality.

We add somewhat more generality if we assume that initially electrostatic conditions prevail and the same uniform fields exist in the lines surrounding the node. (The results are the same if the lines surrounding the node are not occupied with any fields). Using electric field notation, the incident wave amplitude in B is \bar{E}_B and similarly for A, ^+E_A . The fields satisfy $\bar{E}_B = ^+E_B = \bar{E}_A = ^+E_A$. Similar fields apply to the z directed lines. We consider these fields as belonging to the first time step. We then activate the node to start the scattering process.

During the second step the four waves moving away from the node (lines B and B and the two perpendicular lines) will be diminished, thus giving rise to a magnetic field which encircle the displacement current. As before the selected surface element is Δl^2 centered about the node and we can break up the above integral into the four contributions. For example in line B the *change* in displacement current is obtained from, $\epsilon (-E_B^2 - ^+E_B^2) / \Delta t$ and the *superscripts designates the second time step*. Contributions to $^+E_B^2$ may consist of both reflected and transferred (from A) fields. As a result of the difference between the incident wave and the wave moving away from the node, the contribution to the surface integral for this line is then $\{\epsilon (-E_B^2 - ^+E_B^2) / \Delta t\} \Delta l^2$. It is easily verified that

$$(^+H_B^2) \Delta l = \{\epsilon (-E_B^2 - ^+E_B^2) / \Delta t\} \Delta l^2 \tag{1.67a}$$

using the standard TLM relationships for Δt , ^+E_B , ^+H_B , etc... The contributions of the other three lines (line A and the two lines perpendicular

to the paper) are similar but involves the scattered field to the particular line during the second step. In the case of line A, e.g., Eq. (1.67a) becomes

$$\nabla^2_A \Delta l = \{ \epsilon (\bar{E}_A^2 - \bar{E}_A^2) / \Delta t \} \Delta l^2 \quad (1.67b)$$

where \bar{E}_A^2 represents the scattered field from line B to line A during the second step. The curl property for the displacement current is then verified using the same path applied to the conduction current as before. The addition of the fields, in the four lines, is equivalent to the curl property for the magnetic field, at least for the first cell. Just as with Eq.(1.64), however, a 3D treatment is required to demonstrate the equivalence several cells away from the displacement source. In addition, the incorporation of time step changes in the incident fields is straightforward.

In the preceding we have only considered compatibility with the TLM formulation for only one of the two curl equations. The other, $\nabla \times E = -\mu \partial H / \partial t$, has a similar, clear-cut interpretation using the TLM description.

An important point is that with the TLM formulation, although the total field is irrotational at the node, the formulation does in fact yield the correct rotational properties for the various sources, in integral format, about the node. An intriguing feature of Maxwell's Equations, and in particular the curl equations, has to do with its flexibility. In a certain sense we may regard the equations as a "loose" fitting garment which may be filled out to its proper exterior form by any one of several embodiments. Equivalent modes of description include the usual vector analysis, and the iterative equation approach, based on numerical methods or, as in our case, the TLM matrix.

1.16 2D TLM Iteration Method for Nine Cell Core Matrix

As with the 1D approach, we obtain an important relationship, derived from the nature of the 2D node, which relates the field in each line, at a particular time step, to the fields existing in the in the prior time step, both in the same cell and in the surrounding cells. The relationship is obtained with the help of Fig.1.19 which shows a matrix of lines, using as a backdrop a finite difference grid, which we will use later for comparative purposes.

We shall often refer to the nine cell matrix in Fig.1.19 as the *core matrix*. The four TLM lines immediately surrounding the center cell will

be referred to as inner core TLM lines. The remaining eight TLM lines which are labeled we shall refer to as outer core TLM lines. It will be important to observe that the outer core lines form common boundaries with neighboring core matrices. Later, when we compare the TLM results with the finite difference results, we will make use of the fact that the outer core TLM lines will carry less weight than those in the inner core.

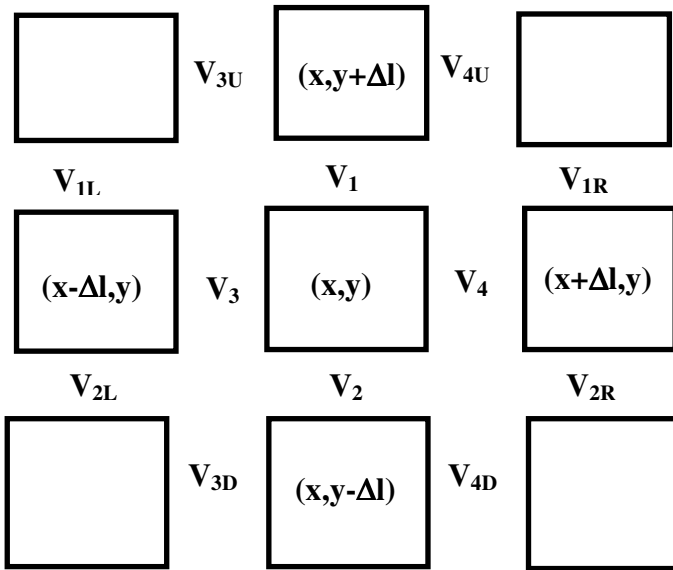


FIG. 1.19 SUPERPOSITION OF TLM MATRIX AND FINITE DIFFERENCE GRIDS USING CORE MATRIX SET.

In examining the TLM formulation of the core matrix, we start with the voltage, V_1 , in line at time $t+\Delta t$. This voltage is the sum of the forward wave, $^+V_1$, and the backward wave, $^-V_1$, with $V_1 = ^+V_1 + ^-V_1$, evaluated at the $t+\Delta t$ time step. How do these voltages relate to the voltages in the prior step at time t ? The forward wave is a result of the of the backward, wave reflected from the left node, and the waves directly transmitted from lines 1L, 3, and 3U. Thus, since the reflection and transfer coefficients are both equal to $1/2$ for a lossless 2D node,

$${}^+V_1(t+\Delta t) = (1/2) {}^-V_1(t) + (1/2)[{}^+V_{1L}(t) - {}^+V_3(t) + {}^-V_{3U}(t)] \quad (1.68)$$

A minus sign in front of ${}^+V_3(t)$ is inserted since, in coupling to line 3, the field direction becomes negative. A similar relation applies to the backward wave in line 1,

$${}^-V_1(t+\Delta t) = (1/2) {}^+V_1(t) + (1/2)[{}^-V_{1R}(t) - {}^-V_{4U}(t) + {}^+V_4(t)] \quad (1.69)$$

The total field at $t+\Delta t$ is

$$V_1(t+\Delta t) = {}^+V_1(t+\Delta t) + {}^-V_1(t+\Delta t) \quad (1.70)$$

In like manner, we calculate $V_2(t+\Delta t)$ in line 2, which is the neighboring line. The two fields, representing lines 1 and 2, are needed in order to make a comparison with the results from the finite difference method. The forward, backward, and total fields in line 2 are:

$${}^+V_2(t+\Delta t) = (1/2) {}^-V_2(t) + (1/2)[{}^+V_{2L}(t) + {}^-V_3(t) - {}^+V_{3D}(t)] \quad (1.71)$$

$${}^-V_2(t+\Delta t) = (1/2) {}^+V_2(t) + (1/2)[{}^-V_{2R}(t) + {}^+V_{4D}(t) - {}^-V_4(t)] \quad (1.72)$$

$$V_2(t+\Delta t) = {}^+V_2(t+\Delta t) + {}^-V_2(t+\Delta t) \quad (1.73)$$

We now form the sum of $V_1(t+\Delta t) + V_2(t+\Delta t)$. We are required to do this since our interest lies in the horizontal field averaged over the two transmission lines, on either side of the cell. $V_1(t+\Delta t) + V_2(t+\Delta t)$ is of course proportional to this average (cell averaged properties are discussed in more detail in the next Chapter). The result is, from Eqs.(1.68)-(1.73),

$$\begin{aligned} V_1(t+\Delta t) + V_2(t+\Delta t) &= (1/2) {}^-V_1(t) + (1/2)[{}^+V_{1L}(t) - {}^+V_3(t) + {}^-V_{3U}(t)] \\ &\quad + (1/2) {}^+V_1(t) + [(1/2)[{}^-V_{1R}(t) - {}^-V_{4U}(t) + {}^+V_4(t)] \\ &\quad + (1/2) {}^-V_2(t) + (1/2)[{}^+V_{2L}(t) + {}^-V_3(t) - {}^+V_{3D}(t)] \\ &\quad + (1/2) {}^+V_2(t) + (1/2)[{}^-V_{2R}(t) + {}^+V_{4D}(t) - {}^-V_4(t)] \end{aligned} \quad (1.74)$$

The above equation is the TLM iteration relating the horizontal fields at $t+\Delta t$ to those at t . The expression simplifies if we assume the system is slightly perturbed, in which case the forward and backward waves in each line are close in value. We can achieve the same results, however, without making such an approximation, by incorporating the reverse iteration. As we have discussed previously, we obtain the reverse iteration by first reversing the propagation directions everywhere, then allowing

the iteration to proceed forward one step, and finally reverting to the original propagation direction. The result is that $V_1(t-\Delta t) + V_2(t-\Delta t)$ is identical to Eq.(1.74) except that wherever we see a forward wave it is replaced by a backward one, and wherever we see a backward wave it is replaced by a forward one. The result is

$$\begin{aligned} V_1(t-\Delta t) + V_2(t-\Delta t) = & (1/2) {}^+V_1(t) + (1/2)[{}^-V_{1L}(t) - {}^-V_3(t) + {}^+V_{3U}(t)] \\ & + (1/2) {}^-V_1(t) + [(1/2)[{}^+V_{1R}(t) - {}^+V_{4U}(t) + {}^-V_4(t)] \\ & + (1/2) {}^+V_2(t) + (1/2)[{}^-V_{2L}(t) + {}^+V_3(t) - {}^-V_{3D}(t)] \\ & + (1/2) {}^-V_2(t) + (1/2)[{}^+V_{2R}(t) + {}^-V_{4D}(t) - {}^+V_4(t)] \end{aligned} \quad (1.75)$$

In order to facilitate the comparison of the TLM result with the finite difference method, we add $V_1(t+\Delta t) + V_2(t+\Delta t)$ to $V_1(t-\Delta t) + V_2(t-\Delta t)$, giving us

$$\begin{aligned} [V_1(t+\Delta t) + V_2(t+\Delta t)] + [V_1(t-\Delta t) + V_2(t-\Delta t)] \\ = [V_1(t) + V_2(t)] + (1/2)[V_{1L}(t) + V_{3U}(t) + V_{1R}(t) - V_{4U}(t)] \\ + [1/2][V_{2L}(t) - V_{3D}(t) + V_{2R}(t) + V_{4D}(t)] \end{aligned} \quad (1.76)$$

Eq.(1.76) is the three tier TLM iteration. Note that the equation does not depend on any forward or backward waves, but only the sums of the two waves in each line. We also remind ourselves that the previous equations apply only to the horizontal lines. In the following we enumerate the similar relations for the transverse lines. Corresponding to Eqs.(1.68)-(1.73),

$${}^+V_3(t+\Delta t) = (1/2) {}^-V_3(t) + (1/2)[{}^+V_{3D}(t) - {}^+V_{2L}(t) + {}^-V_2(t)] \quad (1.77)$$

$${}^-V_3(t+\Delta t) = (1/2) {}^+V_3(t) + (1/2)[{}^-V_{3U}(t) + {}^+V_{1L}(t) - {}^-V_1(t)] \quad (1.78)$$

$$V_3(t+\Delta t) = {}^+V_3(t+\Delta t) + {}^-V_3(t+\Delta t) \quad (1.79)$$

$${}^+V_4(t+\Delta t) = (1/2) {}^-V_4(t) + (1/2)[{}^+V_{4D}(t) - {}^+V_2(t) + {}^-V_{2R}(t)] \quad (1.80)$$

$${}^-V_4(t+\Delta t) = (1/2) {}^+V_4(t) + (1/2)[{}^-V_{4U}(t) + {}^+V_1(t) - {}^-V_{1R}(t)] \quad (1.81)$$

$$V_4(t+\Delta t) = {}^+V_4(t+\Delta t) + {}^-V_4(t+\Delta t) \quad (1.82)$$

As with $V_1(t+\Delta t)$ and $V_2(t+\Delta t)$, we form the sum of $V_3(t+\Delta t)$ and $V_4(t+\Delta t)$:

$$\begin{aligned} V_3(t+\Delta t) + V_4(t+\Delta t) &= (1/2) \text{ }^{-}V_3(t) + (1/2) [\text{ }^{+}V_{3D}(t) - \text{ }^{+}V_{2L}(t) + \text{ }^{-}V_2(t)] \\ &\quad + (1/2) \text{ }^{+}V_3(t) + (1/2) [\text{ }^{-}V_{3U}(t) + \text{ }^{+}V_{1L}(t) - \text{ }^{-}V_1(t)] \\ &\quad + (1/2) \text{ }^{-}V_4(t) + (1/2) [\text{ }^{+}V_{4D}(t) - \text{ }^{+}V_2(t) + \text{ }^{-}V_{2R}(t)] \\ &\quad + (1/2) \text{ }^{+}V_4(t) + (1/2) [\text{ }^{-}V_{4U}(t) + \text{ }^{+}V_1(t) - \text{ }^{-}V_{1R}(t)] \end{aligned} \quad (1.83)$$

The corresponding reverse iteration is

$$\begin{aligned} V_3(t-\Delta t) + V_4(t-\Delta t) &= (1/2) \text{ }^{+}V_3(t) + (1/2) [\text{ }^{-}V_{3D}(t) - \text{ }^{-}V_{2L}(t) + \text{ }^{+}V_2(t)] \\ &\quad + (1/2) \text{ }^{-}V_3(t) + (1/2) [\text{ }^{+}V_{3U}(t) + \text{ }^{-}V_{1L}(t) - \text{ }^{+}V_1(t)] \\ &\quad + (1/2) \text{ }^{+}V_4(t) + (1/2) [\text{ }^{-}V_{4D}(t) - \text{ }^{-}V_2(t) + \text{ }^{+}V_{2R}(t)] \\ &\quad + (1/2) \text{ }^{-}V_4(t) + (1/2) [\text{ }^{+}V_{4U}(t) + \text{ }^{-}V_1(t) - \text{ }^{+}V_{1R}(t)] \end{aligned} \quad (1.84)$$

We then form the three tier iteration by adding $V_3(t+\Delta t) + V_4(t+\Delta t)$ to $V_3(t-\Delta t) + V_4(t-\Delta t)$ to give

$$\begin{aligned} [V_3(t+\Delta t) + V_4(t+\Delta t)] + [V_3(t-\Delta t) + V_4(t-\Delta t)] &= [V_3(t) + V_4(t)] \\ &\quad + (1/2) [V_{3D}(t) + V_{3U}(t) - V_{2L}(t) + V_{1L}(t)] \\ &\quad + (1/2) [V_{4D}(t) + V_{4U}(t) + V_{2R}(t) - V_{1R}(t)] \end{aligned} \quad (1.85)$$

This completes the TLM iterations, consisting of Eqs.(1.76) and (1.85) and their component two tier counterparts, Eqs.(1.74), (1.75), and (1.83) and (1.84).

1.17 2D Finite Difference Method. Comparison with TLM Method

The treatment of the two dimensional problem starts out with the two component wave equations in the x and y directions (without loss). We again use the same core matrix, but now we consider the TLM lines as a backdrop while the finite difference grid is in the foreground. This will help facilitate the comparison of the TLM and finite difference methods. Once the finite difference analysis is completed, we will convert the results to TLM variables, using the core matrix in Fig.1.19.

The two components of the wave equation are:

$$\partial^2 E_Y / \partial x^2 + \partial^2 E_Y / \partial y^2 - (1/v^2) \partial^2 E_Y / \partial t^2 = 0 \quad (1.86)$$

$$\partial^2 E_X / \partial x^2 + \partial^2 E_X / \partial y^2 - (1/v^2) \partial^2 E_X / \partial t^2 = 0 \quad (1.87)$$

Note that the two equations are not decoupled, i.e., because of the presence of the $\partial^2 E_Y/\partial y^2$ and $\partial^2 E_X/\partial x^2$ terms we are no longer dealing with two independent plane wave equations in the x and y directions. A finite difference analysis, similar to that for the 1D case, is carried with the help of the core matrix. Thus,

$$[E_Y(x+\Delta l, y, t) + E_Y(x-\Delta l, y, t) + E_Y(x, y+\Delta l, t) + E_Y(x, y-\Delta l, t) - 4E_Y(x, y, t)]/\Delta l^2 - (1/v^2 \Delta t^2)[E_Y(x, y, t+\Delta t) + E_Y(x, y, t-\Delta t) - 2E_Y(x, y, t)] = 0 \quad (1.88)$$

$$[E_X(x+\Delta l, y, t) + E_X(x-\Delta l, y, t) + E_X(x, y+\Delta l, t) + E_X(x, y-\Delta l, t) - 4E_X(x, y, t)]/\Delta l^2 - (1/v^2 \Delta t^2)[E_X(x, y, t+\Delta t) + E_X(x, y, t-\Delta t) - 2E_X(x, y, t)] = 0 \quad (1.89)$$

In the above equations the difference element is assumed to be the same in both the x and y directions and we set $\Delta x = \Delta y = \Delta l$ with $v = \Delta l/\Delta t$. In order to compare the iterations using the finite difference and transmission line techniques, we solve for the elements $E_X(x, y, t+\Delta t)$ and $E_Y(x, y, t+\Delta t)$, giving

$$E_Y(x, y, t+\Delta t) = E_Y(x+\Delta l, y, t) + E_Y(x-\Delta l, y, t) + E_Y(x, y+\Delta l, t) + E_Y(x, y-\Delta l, t) - 2E_Y(x, y, t) - E_Y(x, y, t-\Delta t) \quad (1.90)$$

$$E_X(x, y, t+\Delta t) = E_X(x+\Delta l, y, t) + E_X(x-\Delta l, y, t) + E_X(x, y+\Delta l, t) + E_X(x, y-\Delta l, t) - 2E_X(x, y, t) - E_X(x, y, t-\Delta t) \quad (1.91)$$

Equations (1.90)-(1.91) give the field elements at time $t+\Delta t$ in terms of prior time elements occurring at $t = t$ and at $t-\Delta t$, and we have chosen $v\Delta t = \Delta l$ in order to simplify the iterations. The selection of Δl is within the allowable range for a stable solution (Reference [5]). The numerical velocity, going from (x, y) to $(x+\Delta l, y+\Delta l)$, is $2^{1/2}\Delta l/\Delta t$. In order to assure a stable solution the wave velocity v must not exceed the numerical velocity. In this case the numerical velocity exceeds the wave velocity by a factor $2^{1/2}$, thus assuring a stable solution.

The following approximations will further simplify the iterative equations,

$$2E_Y(x, y, t) = E_Y(x, y+\Delta l, t) + E_Y(x, y-\Delta l, t) \quad (1.92a)$$

$$2E_Y(x, y, t) = E_Y(x+\Delta l, y, t) + E_Y(x-\Delta l, y, t) \quad (1.92b)$$

$$2E_x(x,y,t) = E_x(x+\Delta l,y,t) + E_x(x-\Delta l,y,t) \quad (1.92c)$$

$$2E_y(x,y,t) = E_y(x,y+\Delta l,t) + E_y(x,y-\Delta l,t) \quad (1.92d)$$

Equations (1.92a)-(1.92b) state that $E_y(x,y,t)$ is the average of the fields at $x+\Delta l$, $x-\Delta l$, $y+\Delta l$, and, and $y-\Delta l$, as suggested by the core matrix. The same type averaging applies to $E_x(x,y,t)$ as well. Substitution of Eqs.(1.92a)-(1.92d) into Eqs.(1.90)-(1.91) then gives

$$E_y(x,y,t+\Delta t) = 2E_y(x,y,t) - E_y(x,y,t-\Delta t) \quad (1.93a)$$

$$E_x(x,y,t+\Delta t) = 2E_x(x,y,t) - E_x(x,y,t-\Delta t) \quad (1.93b)$$

The interpretation of Eqs.(1.93a)-(1.93b) is quite simple. It states that the field at x , y , t is the time average of the fields at times $t+\Delta t$ and $t-\Delta t$. In fact, one may regard the iterative equation as the sum of two independent averaging processes. The first is the spatial averaging of the four cells surrounding (x, y, t) , and the second is the temporal averaging of $t+\Delta t$ and $t-\Delta t$.

At this point, it is convenient to switch over from field variables to TLM variables, in order to facilitate the comparison. The field is assumed to be concentrated in the center of each cell. In order to switch variables, we imagine the cells to be separated from one another by the transmission lines, and for the fields to be concentrated now in the lines, while insuring that the averaging of the fields in the lines reproduces the original field at the center of the cell. Referring to the core matrix, we begin with the fields at the center, $E_x(x,y,t)$ and $E_y(x,y,t)$, which are averaged over the lines, V_3 , V_4 and V_1 , V_2 , respectively, or

$$E_x(x,y,t) = -[V_3(x,y,t) + V_4(x,y,t)]/2\Delta l \quad (1.94a)$$

$$E_y(x,y,t) = -[V_1(x,y,t) + V_2(x,y,t)]/2\Delta l \quad (1.94b)$$

Note that in each case, a distance of $2\Delta l$ is used since the field is averaged over two transmission lines (or two cells). The same definitions also apply to times $t+\Delta t$ and $t-\Delta t$, in which case, we merely substitute the appropriate time in Eqs.(1.94a)-(1.94b). Using the TLM variables, the simplified iterative equations become

$$V_1(t+\Delta t) + V_2(t+\Delta t) = 2[V_1(t) + V_2(t)] - [V_1(t-\Delta t) + V_2(t-\Delta t)] \quad (1.95a)$$

$$V_3(t+\Delta t) + V_4(t+\Delta t) = 2[V_3(t) + V_4(t)] - [V_3(t-\Delta t) + V_4(t-\Delta t)] \quad (1.95b)$$

Equations (1.95a)-(1.95b), however are not very useful since they do not contain any of the “outer” lines such as V_{1R} , V_{3U} , etc., which contribute to the TLM iteration. The outer terms were “lost” when imposing the approximation given in Eq.(1.92). The omission of these terms is an oversimplification. Thus, if we do nothing further we will have succeeded in “approximating away” the problem!

In order to gather in the outer terms, we make a key assumption regarding the fields in the vicinity of the cell. If we select our length parameter, Δl , sufficiently small then we may regard the fields as quasi-conservative over the cell region (rather than the node region), and the TLM variables, which we have substituted for the fields, will indeed behave as voltages. This will allow us to state several important boundary conditions for the core matrix. In order to proceed we utilize Fig.1.20, which applies to the fields $V_1(t)+V_2(t)$. This Figure is similar to Fig.1.19, but now shows three alternate paths going from the $(x,y-\Delta l)$ to $(x,y+\Delta l)$ cell, each of which presumably are equivalent to $[V_1(t) +V_2(t)]$. Each path will have an associated weight factor, with the weights adding up to one. The three paths are listed below.

$$\begin{aligned} \text{PATH A: } & W_1\{V_1(t) + V_2(t)\} = W_1\{A\} \\ \text{PATH B: } & W_2\{V_{4D}(t) + V_{2R}(t) + V_{1R}(t) - V_{4U}(t)\} = W_2\{B\} \\ \text{PATH C: } & W_3\{-V_{3D}(t) + V_{2L}(t) + V_{1L}(t) + V_{3U}(t)\} = W_3\{C\} \end{aligned}$$

W_1, W_2, W_3 are the weights associated with the three paths. We use $\{A\}$, etc... as a shorthand to denote the particular path. We should note that path A is in the inner core of the matrix while B and C are in the outer core. We now make the important assumption that the paths B and C, since they are in the outer core, share equally with its neighbors and therefore W_2 and W_3 have weights half that of W_1 . This is best seen by viewing Fig.1.20 and considering the adjoining 9 cell matrix whose center cell is $(x+2\Delta l, y)$, instead of (x,y) , i.e., consider the new matrix formed by shifting the old matrix two cell length to the right. In this case, the path B TLM lines of the old matrix are shared with the corresponding path C lines belonging to the new matrix. Similar sharing occurs for the original path C. B and C, therefore, should have half the weight of A and thus

$$W_2 = (1/2) W_1, W_3 = (1/2)W_1 \quad (1.96a), (1.96b)$$

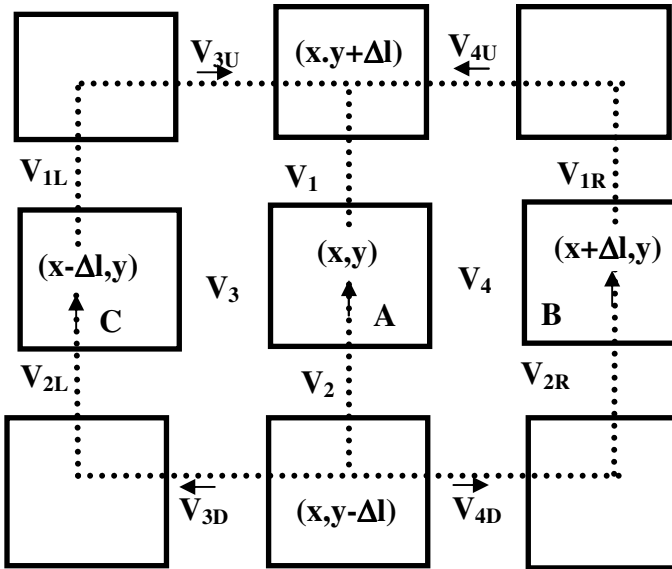


FIG. 1.20 SUPERPOSITION OF TLM AND FINITE DIFFERENCE GRIDS SHOWING THREE POSSIBLE PATHS FOR THE Y DIRECTED FIELD, $V_1(t)+V_2(t)$. PATH A HAS TWICE THE WEIGHT OF B AND C IN THE CORE MATRIX.

where we have assumed that paths B and C are symmetric and thus $W_2 = W_3$. What we still lack, however, are the actual values of the weights. These we can attain from the normalization requirement, by which we demand that the sum of weights equal unity Thus

$$1 = W_1 + W_2 + W_3 \tag{1.97}$$

In view of Eqs.(1.96a) and (1.96b)

$$W_1 = 1/2, W_2 = W_3 = (1/4) \tag{1.98a), (1.98b)}$$

The weight selection has a loose connection to the path lengths of A, B, and C. Since B and C have a path length twice that of A, and the corresponding average fields are therefore half that of A, and this invites the argument that the corresponding weights of B and C should also be half that of A. Although this happens to be the case here, the key factor in obtaining the path weight is related to the neighboring core

matrices and the sharing of the path with its neighbors, discussed further in App (1A.1).

Before proceeding to the decomposition of $[V_1(t) + V_2(t)]$, based on the weights in Eq.(1.98), we should point out that the fact that A, B, and C are not the only possible paths in going from the $(x,y-\Delta y)$ to the $(x,y+\Delta y)$ cells. For example, one possible path not mentioned involves going from $(x, y-\Delta y)$ to $(x+\Delta x,y-\Delta y)$ thence to $(x+\Delta x, y)$ thence to (x,y) and finally to $(x, y+\Delta y)$. Indeed if one allows the path length to grow without limit the there are innumerable number of possible paths. App.1A.1 takes into account the alternative paths, and describes the weighing process involved; the decisive factor in so far as the path weight is concerned, is whether a particular line segment is in the inner core, the outer core, or completely outside the core. Taking into account the higher order paths, however, does not change any of the results. Thus the decomposition of $V_1(t)+V_2(t)$, based on the weights of alternative paths(which go beyond A,B, and C), is identical. We therefore utilize the results of the three paths to decompose $V_1(t)+V_2(t)$. In view of the weights given by Eq.(1.98), the distribution is as follows

$$[V_1(t)+V_2(t)] \rightarrow (1/2)[V_1(t) + V_2(t)] + (1/4)[V_{4D}(t) + V_{2R}(t) + V_{1R}(t) V_{4U}(t)] + (1/4)[-V_{3D}(t) + V_{2L}(t) + V_{1L}(t) + V_{3U}(t)] \quad (1.99)$$

Similar distributions also exist for $V_1(t+\Delta t)+V_2(t+\Delta t)$ and $V_1(t-\Delta t)+V_2(t-\Delta t)$ but since these involve higher order approximations for the *given core matrix*, we will not make us of these relationships. We thus proceed to substitute Eq.(1.99) into Eq.(1.95a), yielding

$$[V_1(t+\Delta t) + V_2(t+\Delta t)] + [V_1(t-\Delta t) + V_2(t-\Delta t)] = [V_1(t) + V_2(t)] + (1/2)[V_{1L}(t) + V_{3U}(t) + V_{1R}(t) - V_{4U}(t)] + (1/2) [V_{2L}(t) - V_{3D}(t) + V_{2R}(t) + V_{4D}(t)] \quad (1.100)$$

But Eq.(1.100) is exactly the TLM iteration given in Eq.(1.76). Equivalently, the substitution of the TLM relations, $V_1(t+\Delta t)+V_2(t+\Delta t)$ and $V_1(t-\Delta t)+V_2(t-\Delta t)$, produces an identity, just as in the 1D case. Again these choices are not mathematically unique. However they are the only functions which physically justify the proper wave motions of the forward and backward waves. A similar averaging leads to the same conclusions for the fields in the x direction, $V_3(t)+V_4(t)$, leading to Eq.(1.85).

In comparing the TLM and numerical approaches, we have not included losses in the 2D treatment, which is very similar to the 1D case. As before, the TLM iterations for the forward and backward motions will not only involve reversing the propagation direction, but will also involve, in the case of the reverse iteration, the conversion of the resistive loss into a gain factor. As with the 1D case, the TLM and Finite Difference methods for 2D, including losses, lead to identical results. In addition we have not discussed what happens when the region is non-uniform and thus TLM lines in the same vicinity will have different line lengths (due to differing dielectric constants). Although the basic approach is the same, this issue cannot be addressed unless concepts such as “nearest nodes”, discussed in Chapter 5, are introduced.

To summarize, the identity of the TLM and finite difference results should not be surprising, since we insisted that the cell size (or, alternatively, the time step) is sufficiently small, so that, at least locally, the fields are conservative about the node region. To be sure the curl equations are satisfied, as indicated in Section 1.15. The numerical technique of finite differences is therefore consistent with the iteration based on transmission line concepts. In a mathematical sense, the transmission line approach is closely related to a particular finite difference method, of which there are many, differing mainly in the speed of convergence or in program complexity. An important advantage of the TLM iteration is the fact alluded to previously, namely, it involves only two time steps and is therefore easier to apply. Other advantages of the TLM method, as mentioned previously, are the powerful physical and intuitive understanding which may be brought to bear on a wide spectrum of electromagnetic problems. With the TLM method, any mathematical changes made in a computer code have an immediate physical interpretation. Conversely, any physical changes in a problem are easier to implement in the TLM iteration code.

1.18 Final comments: Inclusion of Time Varying Signals and Phase Coherence

Thus far we have only considered unipolar signals with uniform amplitudes and a step risetime. For the sake of simplicity this simple type signal is assumed almost exclusively throughout the book. Indeed most of the important properties of the TLM approach may be obtained in this manner. The behavior of more complex time varying signals may be obtained by selecting a sufficiently high density matrix. One can then

approximate the signal with a series of pulses. The pulsewidth of each pulse is set equal to the TLM width.

An important example of a time varying signal is that of consecutive short pulses of alternating polarity, which may then be used to approximate an AC signal (see Chapter 7, Section 7.12). As pointed out in Section 1.14, multiple signals incident on a node do not introduce any fundamental changes since the outputs may be added in linear fashion, despite the complexity of the signals.

An important property of a signal is whether and how it reacts to the presence of a signal in a neighboring TLM line. The signals need not be necessarily time varying but may be constant in amplitude as well. The phase coherence of the signals over a particular region, which may be considered the result of the correlation of the signals, affects the way such signals scatter and is discussed in Chapter 5.

APPENDICES

App.1A.1. Effect of Additional Paths on Weighing Process

We saw in Section(1.17) that paths B and C, by virtue of the fact that they traversed TLM lines in the outer core, possessed weights half that of the core path A.

This arises because the outer core lines are shared with similar neighboring core matrices and therefore their weight is reduced by a factor of two.

In Section (1.17) we considered only the three most “obvious” paths in going from cell $(x,y-\Delta l)$ to $(x,y+\Delta l)$. As one might guess, there are any number of paths between these two cells. We should identify however the paths which accomplish the traversal using the minimum number of cell lengths. Indeed there are four additional paths, consisting of four cell lengths each, which we have thus far not yet specified. These four, in addition to paths B and C, make up all the paths consisting of four cell lengths. The four new paths, which go from cell $(x,y-\Delta l)$ to $(x,y+\Delta l)$, representing $V_1(t) + V_2(t)$, are

$$\text{Path G: } (x, y-\Delta l) \rightarrow (x+\Delta l, y-\Delta l) \rightarrow (x+\Delta l, y) \rightarrow (x, y) \rightarrow (x, y+\Delta l) \quad (1A.1a)$$

$$\text{Path H: } (x, y-\Delta l) \rightarrow (x, y) \rightarrow (x+\Delta l, y) \rightarrow (x+\Delta l, y+\Delta l) \rightarrow (x, y+\Delta l) \quad (1A.1b)$$

$$\text{Path I: } (x, y-\Delta l) \rightarrow (x-\Delta l, y-\Delta l) \rightarrow (x-\Delta l, y) \rightarrow (x, y) \rightarrow (x, y+\Delta l) \quad (1A.1c)$$

$$\text{Path J: } (x, y-\Delta l) \rightarrow (x, y) \rightarrow (x-\Delta l, y) \rightarrow (x-\Delta l, y+\Delta l) \rightarrow (x, y+\Delta l) \quad (1A.1d)$$

These four paths will actually have more weight than B or C since in each case one of the segments involves crossing an inner core TLM line.

We now consider all seven paths (A, B, C, G, H, I, J) in the weighing process. We symbolically make the following decomposition of $V_1(t) + V_2(t)$,

$$\begin{aligned} V_1(t) + V_2(t) = & W_1\{A\} + W_2\{B\} + W_2\{C\} + W_3\{G\} \\ & + W_3\{H\} + W_3\{I\} + W_3\{J\} \end{aligned} \quad (1A.2)$$

We have implicitly made the assumption that the weights for G,H,I,J are all equal, given by W_3 . As we have noted previously the paths B and C traverse only outer core lines and therefore $W_2 = W_1/2$. The remaining four paths are slightly more complicated. As noted in Eq.(1A.1), the paths traverse *both* inner and outer core lines. In particular one of the four line segments comprising each path belongs to an inner core while the other three belong to the outer core. We therefore define the weight of each one of these paths as

$$\begin{aligned} W_3 = AV[W_3] &= (1/4)[(W_1/2) + (W_1/2) + (W_1/2) + (W_1)] \\ &= (5/8)W_1 \end{aligned} \quad (1A.3)$$

Note that the weight of these paths exceeds that of B or C, which arises from the fact that these paths traverse an inner core line rather than an outer one. Also note that the differences in weight exist despite the identical length (four cell lengths) for both types of paths.

Having assigned weights, relative to W_1 , we must now determine W_1 , and therefore all the other weights, by requiring the weights to be normalized. Thus

$$\begin{aligned} 1 = & W_1 + [(W_1/2) + (W_1/2)] \\ & + [(5/8)W_1 + (5/8)W_1 + (5/8)W_1 + (5/8)W_1] \end{aligned} \quad (1A.4)$$

where W_1 is the weight assigned to A, $W_1/2$ is the weight for B and C, and $(5/8)W_1$ is the weight for G, H, I, and J. Solving for W_1 ,

$$W_1 = 2/9 \quad (1A.5)$$

Since $W_2 = (1/2) W_1$ and $W_3 = (5/8)W_1$

$$W_2 = 1/9; \quad W_3 = 5/36 \quad (1A.6a), (1A.6b)$$

Before determining the distribution of $V_1(t)+V_2(t)$, resulting from the path weights, it will be convenient to note that the combination of certain paths simplifies the results. In particular,

$$\{G\}+\{H\} \rightarrow \{A\}+\{B\} \quad (1A.7a)$$

$$\{I\}+\{J\} \rightarrow \{A\}+\{C\} \quad (1A.7b)$$

Eq.(1A.7a) comes about because of the cancellation of $V_4(t)$ when adding paths G and H, leaving $\{A\}$ and $\{B\}$ terms. Similarly, $V_3(t)$ cancels in Eq.(1A.7b) when adding paths I and J, leaving $\{A\}$ and $\{C\}$. At this point we can ascertain the distribution of $V_1(t)+V_2(t)$. Combining Eqs.(1A.2)-(1A.7), we have

$$V_1(t) + V_2(t) \rightarrow [W_1+2W_3]\{A\} + [W_2+W_3]\{B\} + [W_2+W_3]\{C\} \quad (1A.8)$$

Combining above and the weight values, $W_1=2/9$ $W_2=1/9$ $W_3=5/36$, we have

$$V_1(t) + V_2(t) \rightarrow (1/2)\{A\} + (1/4)\{B\} + (1/4)\{C\} \quad (1A.9)$$

The distribution for all seven paths is therefore the same as that obtained solely from the paths $\{A\}$, $\{B\}$, and $\{C\}$

Use of Paths G, H, I, J Alone as an Independent Set

In simply adding the four paths G, H, I, J to A, B, and C, and then going through the normalization process to obtain the weight distribution, we have actually done twice the amount of work that is really necessary. This is because G, H, I, and J form an independent set so far as describing the various paths $(x,y-\Delta l) \rightarrow (x,y+\Delta l)$ is concerned. This is because of the relationships, Eqs.(1A.7a)-(1A.7b)), which show that A, B, and C may be expressed by combinations of G,H,I and J. As before we first find the weight W of each of the four paths; in this case the job is simple since they are all identical. Thus

$$W = 1/4 \quad [\text{Paths G, H, I, J only}] \quad (1A.10)$$

If we now simply express $(x,y-\Delta y) \rightarrow (x,y+\Delta y)$ in terms of these variables we have

$$V_1(t) + V_2(t) \rightarrow (1/4)[\{G\}+\{H\}+\{I\}+\{J\}] \quad (1A.11)$$

or, referring to Eq.(1A.7),

$$\begin{aligned} [V_1(t)+V_2(t)] &\rightarrow (1/4)[2\{A\}+\{B\}+\{C\}] \\ &\rightarrow (1/2)\{A\}+(1/4)\{B\}+(1/4)\{C\} \end{aligned} \quad (1A.12)$$

But this is exactly the same result used when considering only A, B and C (or all seven paths at the same time). The result leads once more directly to Eqs.(1.76) and analogously to Eq.(1.85).

We have thus exhausted all the possibilities for paths up to four cell lengths. We can then perform the same type of procedure for path lengths of six cell lengths, but no new results or information are obtained. We should also add that as we go to paths of six cell segments or longer, then some of the paths will go outside the core matrix; for these paths any line segments outside the core matrix are considered to have zero weight.

App.1A.2. Novel Applications of TLM Method: Description of Neurological Activity Using the TLM Method

Electromagnetics, of course, is not the only field where the TLM method may be employed. Acoustic wave motion (or any phenomena governed by a wave equation) and heat diffusion are examples of other technologies where the TLM matrix method may be utilized. In fact, the electromagnetics application is probably more difficult to incorporate into the TLM formulation because of the vector nature of the field and because of the dual polarization associated with the wave. Aside from the area of physics, however, there is a branch in the biological sciences to which the TLM method appears to have a natural affinity. The possible application is the functioning of the brain, which relies on a vast array of nerve fibers and synapses, analogous to the transmission lines and nodes of the TLM matrix.

Analogy of TLM Method and Neurological Activity

We *speculate* here how the TLM method may be used as a framework to describe neurological activity, in particular that of the brain. As we have mentioned, in the area of nerve cells the nerve fibers and synapses appear to play a role similar to transmission lines and nodal switches

in the TLM model. Nerve impulses are conveyed along the fibers. The synapses exist at the juncture of two or more fibers and they serve to control the flow of the impulses from one fiber to another. The nature of the impulse propagation along the fibers is discussed briefly in [6]. In the case of the brain, the degree of activation of a particular node, and its location, are probably central to the thought process. The activation of a particular region of synapses, or else the simultaneous activation of several regions, may be interpreted by the brain as a sensation or thought. Further the activation of one or more regions may contribute to the activation of an entirely new region. During non-waking hours, particular (or even most) synapses may be activated or “tuned up” periodically to maintain functionality. The “recharging” of a node (and its associated fibers) also is of considerable importance. Ultimately, how fast these nodes can be recharged will affect the speed with which thought processes can be handled. Other factors affecting speed, in analogy with ordinary physical processes, include the speed with which signals are conducted along the neurons, and the “switching speed” of the synapses. One can only speculate about the creative process within the brain. It is quite possible that random and frequent activations of various regions in the brain occur all the time. A healthy brain has the ability to recognize a particular type of node activation (i.e., a thought or idea) as a “solution to a problem” or as the starting point of an entirely new concept. Most of the time these activations come and go without being recognized for their potential value. Memory storage may be regarded, within the TLM framework, as the charging up of a particular cell (node and line), or even a region of the TLM matrix, beyond some threshold value. Stored information is retrieved by activation of the node or region of nodes. The activation of a particular region may trigger other near-by regions, thus giving rise to a flood of related memories. The brain also appears to rely on redundancy, so that multiple regions throughout the brain produce the same memory when activated. It is quite possible that the strength of a particular memory may depend as much on the number of redundant sites, rather than the strength of a particular site. The simultaneous activation of these regions, acting in “parallel”, then contributes to the strength of the memory. With time, the particular memory fades unless periodically activated. The memory dimming may be brought about perhaps by the decline of the number of sites as well as the strength of the individual sites, which produce the memory.

There is also the conjectural possibility of correlation among signals traveling along neighboring nerve fibers. Chapter 5 deals with the topic of correlation between waves in neighboring TLM lines; such correlations drastically affect the wave scattering, wherein the correlated signals move as a group and with less transverse scattering. By analogy, correlations within the brain (assuming they exist) may allow neighboring signals to travel as a group along paths which represent a kind of “shortcut”. We may regard the wave correlations as giving rise to “hunches” or intuitive ideas. Again, we stress that wave correlation among nerve fibers is an untested idea, although Penrose [6] has speculated on the role of a revised quantum theory in explaining brain activity.

These and other speculations concerning impulses in the brain are very adaptable to the TLM matrix model. The speculations mentioned in the previous discussion may be quantified using the TLM formulation. The application of the TLM matrix may be regarded either as a model or alternatively as a handy and adaptable mathematical tool for the transmission of information contained in nerve impulses. Regarded as a model, one must then obtain predictions of TLM model and compare these with experimental observations. Of course the nerve fibers do not form neat geometrical shapes, such as cubes or hexagons, as we assume in TLM analysis. The actual fibers appear as a tangled array with irregular shapes and with varying fiber lengths. Despite these differences, the same type of analysis may be applied to nerve impulses, taking into account the random nature of the fiber shape and length. In some ways the irregularity of the fibers is an advantage since it removes the anisotropy associated with the symmetry elements, where the energy is constrained to flow in only certain directions. With an irregular cell matrix, we are not bound to a preferred direction. We will see in later Chapters how this anisotropy is removed from the symmetry elements.

REFERENCES

1. H Bertoni, L. Carin, and L. Felsen, *Ultra-Wideband, Short-Pulse Electromagnetics*, Plenum Press, New York, 1993.
2. L. Carin and L. Felsen, *Ultra-Wideband, Short-Pulse Electromagnetics 2*, Plenum Press, New York, 1995.
3. W. Panofsky, and M. Philips, *Classical Electricity and Magnetism*, Addison Wesley, Reading, Mass., 1962.

- 4 W. Johnson, *Transmission Lines and Networks*, McGraw Hill, New York, 1950.
5. R. Haberman, *Elementary Applied Partial Differential Equations*, Prentice Hall, Englewood Cliffs, N.J., 1987.
6. R. Penrose, *The Emperor's New Mind*, Oxford University Press, New York, 1989.